maxell

A study of the physical properties of high density Magneto-Optical media

Why does MAMMOS ("Magnetically Amplified Magneto-Optical System") work?

Manuel Bilderbeek

26th April 2001

Master's Thesis
Department of Solid State Physics 2
University of Nijmegen
The Netherlands

maxell

A study of the physical properties of high density Magneto-Optical media

Why does MAMMOS ("Magnetically Amplified Magneto-Optical System") work?

Manuel Bilderbeek

26th April 2001

Master's Thesis
Department of Solid State Physics 2
University of Nijmegen
The Netherlands

Preface

In September 1995 I started as a physics student at the University of Nijmegen (we are not allowed to say "Catholic University of Nijmegen"...). After some struggling in the first year—I underestimated how much one should do in the second semester—which caused about one year of delay, everything went smoothly. There was even some extra time for some additional courses due to that delay. Finally, in September 1999 I started on my "graduation-work" in the department of Experimental Solid State Physics 2.

I really looked forward to this, since it was something completely different: no lectures and examinations, but really working on a research project. It has its good sides and bad sides though. The bad sides are e.g., 1) that sometimes you have to wait a long time (e.g., before your measurement is finished, or before some equipment is free or found), 2) that it is hard to understand what you're doing sometimes, 3) that you have to read a lot of articles, because you discover you hardly know anything in-depth about any topic, etc. But on the other hand there is a lot one learns in such a period. And one can have the possibility to go somewhere one doesn't get so easily, in my case: Japan. I was very happy that I was given the opportunity to have a $3\frac{1}{2}$ month external internship at Hitachi-Maxell in Japan. It enabled me to learn even more and not only about physics.

So what have I been doing all that time then? Well, the story is as follows. When I came to Prof. Theo Rasing around September 1999 to inquire about the possibilities for graduation work at his department, he told me that he had just had visitors from Japan. Those were the people from Hitachi-Maxell. They had asked Theo if his department would be interested in measuring some properties of their new MAMMOS (Magnetically Amplified Magneto-Optical System: a new way of reading out the information from a magneto-optical (cf. MiniDisc) disk with a very high recorded data density) disks. As a matter of fact, they wanted to know how fast a magnetic domain wall can expand in such a disk, which is determining the read-out speed of MAMMOS.

This sounded interesting to me. But of course I also immediately asked Theo if I could go to Japan for some time too, for the external part of my graduation work. Theo said that he thought it would be no problem to arrange that. And, after some consideration, I decided this was a good choice for my graduation work.

I started to dive into literature and discovered bit by bit how this MAMMOS was supposed to work. Luckily, after about two months, a new postdoc came to our department: Julius Hohlfeld. He was asked to join me on this project. In fact, he was my 'mentor' since then. After he came, things became clearer. First he wanted to do some measurements of his own interest and after that we

started to make a set up to look at MAMMOS, of which we got one sample from Japan. I did some preliminary measurements on it. After that we were also getting somewhere with the main measurements, thanks to Julius' experience. It was really going well at the moment it was time for me to go to Japan. This was by the way easier said than done, there were some problems getting a visa... But after that was cleared up, I went to Japan, flying into adventure.

I had a great time there! From all e-mails I sent from Japan, I composed an e-mail diary. At the moment I am still working on it, but it is almost complete. This diary will be available for anyone who is interested in my experiences in Japan. As far as physics is concerned: the main thing I did there was looking at magnetic domains in MAMMOS disks with a microscope.

When I came back, it appeared that the most important measurements on the set up in Nijmegen had been done while I was away. That was of course a bit disappointing. But on the other hand: the results were quite interesting and Julius was even writing an article about them for a very good magazine!

Being back in Nijmegen, I had a hard time finishing my work. I had to write everything I had done down in this Master's Thesis. It took me a while to get started, because I was loaded with lots of data and information, without any structure. Yes, it took me some time, but with the help of the people in the department and others who put me to it, I finally started to get things done. I collected the necessary information, did some additional measurements and wrote the thesis. The result lies in front of you!

Note that the final goal of the project has not been reached yet, but we have made big steps towards it so that in the near future this expansion speed can be measured.

To conclude I want to thank a number of people. First of all the people of the department for their support and patience: Theo (for keeping faith in me, helping and arranging everything, including the internship in Japan), Julius (for being my mentor and teaching me so much), Anthony (for helping me out many times, teaching me things, etc.) and the others. They know who they are! I of course also thank everyone who made my stay in Japan possible and pleasant, especially: Dr. Ohta (for allowing me to come to his laboratory), Dr. Awano (for so many things I can't possibly start to list them!), Mr. Tani (for helping me out, keeping me company, etc.) and the rest of the MAMMOS group (Mr. Imai, Mr. Sekine, Mrs. Inoue) for helping me with problems, showing me things, etc., etc. Also thanks to other Maxell people for making my time more enjoyable: Mr. Inaba (photographs, trips, entertainment), Mr. Ido (talking, trips), Mr. Nose (for taking me to Tsukuba, Nikko and Narita Airport), the people of the English class: Michael (a great host!), Mr. Kouda, Mr. Uebayashi, Mr. Matsuda and the others. Special thanks to Meiko Takeuchi for being such a great friend. To all of you: どうもありがとうございました!

Finally, I also want to thank my family and Anke for their great support!

I have most likely forgotten people here, but you must know that I am grateful to you!

Manuel Bilderbeek
(a.k.a. マニュエル ビルデルベーク)
Nijmegen, 9th April 2001

This document was typeset using LaTeX 2ε.

Voorwoord

Hier dan de Nederlandse versie van het voorwoord. Het is gebruikelijk het voorwoord alleen in de moedertaal te schrijven, maar ik heb het hier in zowel het Engels als het Nederlands gedaan, omdat de hele scriptie in het Engels is. En dan vind ik het vreemd dat het voorwoord ineens in het Nederlands is. Maar omdat niet iedereen zo goed is in het Engels en men toch misschien interesse in het voorwoord heeft, heb ik ook deze vertaling opgenomen.

In ieder geval... In september 1995 ben ik begonnen als natuurkunde student aan de KUN. Na wat problemen in het eerste jaar—ik had het tweede semester een beetje onderschat—is alles vrij vlot verlopen. Ik heb zelfs wat extra vakken kunnen doen, omdat ik hier en daar vroegere vakken moest inhalen en nog geen vakken van het toen huidige jaar kon doen. Uiteindelijk ben ik in september 1999 met het afdelingswerk begonnen aan de afdeling Experimentele Vaste Stoffysica 2.

Ik had hier echt naar uitgekeken, omdat het zo anders was dan gewoon vakken volgen en tentamen doen. Hier kon ik echt aan de slag. Het werken op zo'n afdeling heeft echter zijn voor- en zijn nadelen. Nadelen zijn bijvoorbeeld 1) dat je soms lang moet wachten (totdat je meting is afgelopen of er bepaalde apparaten beschikbaar of gevonden zijn), 2) het soms moeilijk is te begrijpen waar je nu eigenlijk mee bezig bent en 3) dat je in het begin enorm veel moet lezen, omdat je erachter komt dat je eigenlijk niets weet van specialistische onderwerpen. Maar aan de andere kant heb ik ook enorm veel geleerd, zowel praktisch als theoretisch. En een ander voordeel is dat je de kans kunt krijgen ergens heen te gaan waar je normaal nooit heen gegaan zou zijn; in mijn geval: Japan. Ik was erg blij dat ik de kans gekregen heb om $3\frac{1}{2}$ maand stage te lopen bij Hitachi-Maxell in Japan. Ik heb daar heel veel geleerd en niet alleen over fysica.

Maar wat heb ik dan de hele tijd gedaan? Het zit als volgt. Toen ik in september 1999 bij Theo Rasing kwam om te vragen of hij nog een leuk afstudeerproject had, vertelde hij me dat er net mensen uit Japan op bezoek waren geweest. Dit bleken de mensen van Hitachi-Maxell te zijn. Ze hadden gevraagd of de afdeling geinteresseerd was om bepaalde eigenschappen van hun nieuwe MAMMOS (Magnetically Amplified Magneto-Optical System: Magnetisch versterkt magneto-optisch systeem, een nieuwe manier om data die met een heel hoge dichtheid is opgenomen op een magneto-optisch medium (MiniDisc is bijvoorbeeld ook gebaseerd op magneto-optica) uit te kunnen lezen) schijfjes te meten. Preciezer gezegd: ze wilden weten hoe snel een magnetisch domein kan groeien in zo'n schijfje, wat van belang is om te kijken hoe snel MAMMOS kan werken.

Dit klonk interessant in mijn oren. Maar natuurlijk heb ik ook direct ge-

vraagd of het mogelijk zou zijn om dan ook mijn externe stage in Japan te lopen. Volgens Theo was dit wel te regelen en na een paar dagen nagedacht te hebben, ben ik dus mijn afstudeerwerk op deze afdeling begonnen.

Ik begon met in de literatuur te duiken en ontdekte stukje voor stukje hoe MAMMOS in elkaar zat. Gelukkig kreeg ik na een maand of twee versterking in de vorm van een nieuwe postdoc: Julius Hohlfeld. Hij is toen mijn directe begeleider geworden en heeft zich ook in MAMMOS verdiept. Hij wilde echter eerst wat metingen voor een eigen onderzoek doen, maar daarna zijn we begonnen met een opstelling om eigenschappen van MAMMOS schijfjes te meten. Intussen hadden we al een sample uit Japan gekregen. Ik heb daar toen wat kleinere hulpmetingen aan gedaan. Maar door de ervaring van Julius ging het met de 'hoofdmetingen' ook al redelijk goed. En op het moment dat het pas echt begon te lopen, was het tijd om naar Japan te gaan. Dit ging trouwens ook niet zonder slag of stoot: er waren wat problemen met het krijgen van een visum... maar toen dit opgelost was, ging ik naar Japan—het avontuur in.

Het was een fantastische ervaring! Van alle e-mails die ik uit Japan verstuurd heb, is een soort dagboek gemaakt. Daar ben ik nu nog steeds mee bezig, maar het is bijna af. Mensen die interesse hebben in mijn belevenissen in Japan, kunnen het bij mij verkrijgen. Wat natuurkunde betreft: in Japan heb ik voornamelijk met een microscoop gekeken naar magnetische domeinen in die MAMMOS schijfjes.

Toen ik terug kwam, bleek dat de belangrijkste metingen gedaan waren terwijl ik in Japan was. Dat was natuurlijk een beetje teleurstellend. Maar aan de andere kant waren de resultaten zodanig interessant dat Julius er een artikel over aan het schrijven was voor een vooraanstaand tijdschrift!

Eénmaal terug in Nijmegen viel het behoorlijk tegen om mijn afstudeerwerk af te ronden. Ik moest al mijn resultaten netjes opschrijven in deze scriptie. Het duurde even voordat ik daadwerkelijk begon, omdat ik overladen was met gegevens en resultaten van allerlei soort. Na een tijdje lukte het toch—dankzij mensen op de afdeling en andere stimuli—om de boel een beetje op een rijtje te krijgen. Ik ordende de informatie, haalde eruit wat er uit te halen viel, deed wat extra metingen en schreef het op in een scriptie. Het resultaat ligt voor je!

Overigens is het doel van het hele project nog niet bereikt, maar er zijn al wel flinke stappen gemaakt die zorgen dat er binnen korte termijn echt naar die expansiesnelheid gekeken kan worden.

Als laatste nog een (verkort t.o.v. de Engelse versie) dankwoord. Ten eerste voor alle mensen van de afdeling voor hun geduld en ondersteuning: Theo, Julius, Anthony en de anderen. Zij weten wie ik bedoel! Natuurlijk dank ik ook degenen die mijn verblijf in Japan mogelijk en plezierig gemaakt hebben, vooral: Dr. Ohta, Dr. Awano, Mr. Tani en de rest van de MAMMOS groep (Mr. Imai, Mr. Sekine, Mrs. Inoue). Ook dank aan de andere Maxell mensen voor het leuker maken van mijn verblijf in Japan: Mr. Inaba, Mr. Ido, Mr. Nose, de mensen van English class: Michael, Mr. Kouda, Mr. Uebayashi, Mr. Matsuda en de anderen. Ook dank ik Meiko Takeuchi voor het feit dat ze zo'n goede vriendin is. Voor allemaal: どうもありがとうございました!

Tenslotte wil ik mijn familie en Anke bedanken voor hun geweldige ondersteuning.

En ik ben ongetwijfeld mensen vergeten, maar zij weten vast dat ik ze erg dankbaar ben!

Manuel Bilderbeek
(alias マニュエル ビルデルベーク)
Nijmegen, 9 april 2001

Contents

Chapter 1

Introduction

Data recording has a long history. The biggest part of it is recording just by ink on paper—or a similar recording medium. However, as we move in history to the present day, the methods of recording appear to have advanced in an exponential way. Think of the first analog recordings with the gramophone: vibrations were recorded on a roll by a scratching needle. The first magnetic recording emerged in the 1940s. This was still audio-only. The resulting tape recording techniques still prevail today, although they are getting less and less popular since there are much better alternatives nowadays. Later the technology of tape recording was extended to make video recording possible. The preliminary techniques for this were already invented in 1956, but it took until the mid-seventies until low-cost consumer products appeared on the market.

At the end of the 1970s computers became more and more mature, which triggered the development of digital data storage media. However, the important inventions were already done much earlier. The rotating rigid disk for digital data storage was an innovation done in 1957 already. The flexible disk was realized in the mid-seventies—indeed mainly for use on personal computers. Also for this technology we can say it is still in use today.

Although the disk is most common today, a long time only digital tapes were used for data storage, mainly for back up of computer files. This technology has been popular for a long time. Even today big archives are made on tape. It is recognized though that for other purposes than archiving, tape is too limited, since the information can only be accessed sequentially.

Both for disk as well as for tape storage media, there has been a great development with time. Not only the media itself improved, but also the heads and the electronics, resulting in an increasing linear and track data density, higher data transfer rate and shorter access times. To give an example: the capacity of the hard-disk drives has roughly doubled every year since 1957. This is illustrated in a graph made by IBM, see figure 1.1.

Since 1985 there is a new invention in the recording business: optical-beam storage technology, in short: Magneto Optical (MO) technology. It makes use of a laser beam to read out magnetically stored data via the Magneto Optical Kerr Effect (MOKE, see also section 2.6.1). The big advantages are that it is a non-contact method—meaning less wear of components and less sensitive for dirt—and the recording density can be increased until the diffraction limit. This also enables the medium to be removable. So the removableness of the floppy

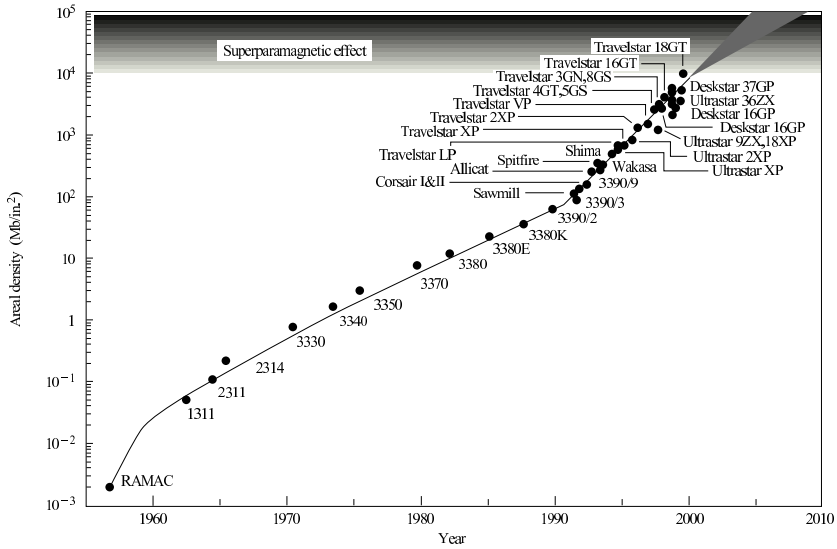

Figure 1.1: The exponential growth of the areal bit density of hard disk drives made by IBM. The names and numbers refer to the models.

is combined with the main features of the hard disk (i.e., high capacity, high data-transfer rate, rapid access).

But of course existing techniques can almost always be improved. In the meantime many improvements have been made to MO recording, mainly to increase the data density. Smart ways of recording and even smarter ways to read out the bits have been invented, which make it possible to go beyond the diffraction limit with the bit density. The research presented in this thesis is meant to contribute to the research of one of the newest MO developments: MAMMOS, the Magnetically AMplified Magneto Optical System.

1.1 MO recording and readout

Conventional MO recording and readout is based on a relatively simple mechanism. Recording is done by focusing a laser spot on the disk, which increases the temperature locally. This decreases the coercivity of the magnetic layer so that an external field can write the desired magnetic information. There is no problem with the size of the coil, since area affected by the field can be arbitrarily large: only the heated part of the medium is influenced by it. See figure 1.2.

The readout is in principle no more than using the Kerr effect (which is a rotation in the polarization of the incident light when it is reflected on a magnetized medium, see below). The incident polarized laser beam is focused on the disk and the reflected light is led through an analyzer to detect the rotation of the polarization. Depending on the magnetization the rotation is clockwise or anti-clockwise, which is translated in a strong or a weak signal transmitted through the analyzer. See section 2.6.1 for a more thorough explanation of

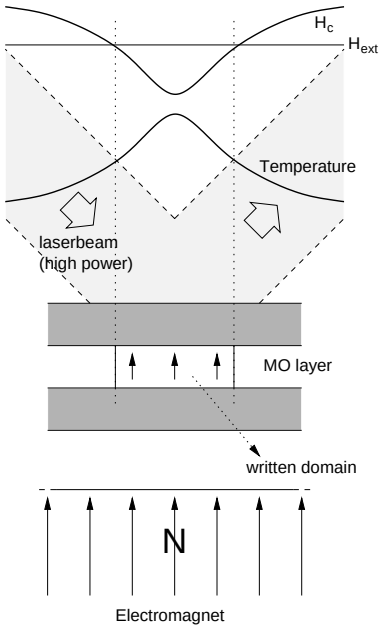

Figure 1.2: Schematical view of MO recording. The heating of the laser beam locally decreases the coercivity of the MO layer, enabling the external field to magnetize it there.

MOKE. During readout, the laser beam power is of course a lot lower than when writing, so that there is no significant change in temperature and thus no effect on the recorded information.

A practical problem is tracking and focusing. If the disk does not rotate around its actual center, this will make the track of bits wobble around a certain mean radius. Also, the disk may wobble in the z-direction, as a result of the high rotation speed. To correct for this, auto focus and auto tracking is applied. For the latter it is needed to make a land and groove structure on the disk, i.e., a zig-zag surface (as seen in a cross section) having one track on the 'groove' and the adjacent track on the 'land'. This is illustrated in figure 1.3. By using the diffraction pattern of the disk's surface, one can get a tracking error signal with which one can correct the position of the read out head. Auto focus can be acquired by using a collimating lens, a knife edge and a split diode pair. When the beam is focused, both diodes will receive an equal amount of light, but when the beam is getting out of focus, this balance shifts. More detailed information about this can be found in e.g. [1].

The limit of conventional MO is of course that the bit size can never be smaller than the laser spot size. Writing higher densities is not a big problem: simplistically speaking, you can just overlap previous 'bits' (see figure 1.4 for an illustration of this), which results in a minimum bit size of about only 20 nm. However, the limit is of course very noticeable when trying to read out the recorded bits, as the MO signal is proportional to the bit size and several bits will be in the read out laser spot (they are not resolved) leading to an average signal of around zero. To counter this limit, several solutions have been proposed,

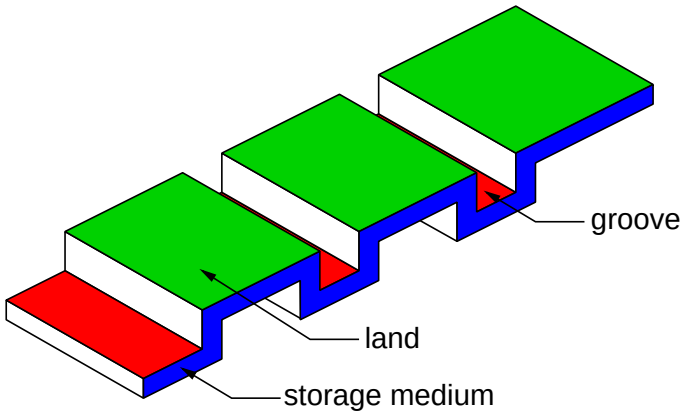

Figure 1.3: Lands and grooves in an optical disk. In this example the zig-zag pattern is 'square', but also triangular or trapezium shapes are possible. It is needed for auto tracking in MO readout systems.

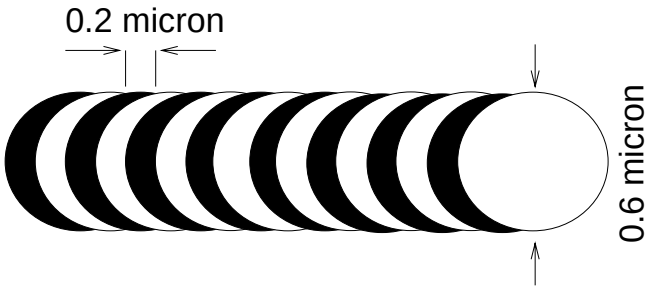

Figure 1.4: An example of how high bit densities can be written on a disk. The consecutive bits are partly overwriting each other. The dimensions given are an example.

amongst which MSR (Magnetic Super Resolution, which is already commercially used at the moment) and MAMMOS. This research is focused on the MAMMOS solution, which is at the moment still in development.

In MAMMOS, the Magnetically Amplified Magneto-Optical System, the read out problem is overcome by using a double layer structure. In the recording layer the very small bits are recorded. During read out, those bits are copied to the read out layer and there expanded (magnified) by an external field to a size that can be even bigger than the laser spot size. This enables the system to get a saturated signal in stead of a very weak signal of the original small recorded bits. This idea was first proposed by Awano *et al* of Hitachi-Maxell Ltd in 1996 [2].

This is a very short description of the general idea of MAMMOS, see below for more.

1.2 Goals

This research was started with the goal to find out the expansion speed of the magnetic domains in the readout layer, as higher bit densities also demand high transfer rates. This can be split up in the following subgoals:

- find out how fast the magnetization can be destroyed (which is also interesting for recording if this is investigated on the recording layer, since it is part of the writing process)
- measure magnetization reversal time
- measure expansion speed of copied domains, with ultrafast microscopy, for example

However, the first two subgoals took enough time and effort to fill this master's thesis. The time resolved microscopy is not done yet at the moment.

Except for those two subgoals, there was also a general goal: get as much information as possible on the MAMMOS media... There is still very little known about them.

Chapter 2

Theory

2.1 Introduction to (ferro)magnetism

As an introduction to magnetism, the main properties and characteristics of ferromagnets are presented in this section. Also some main concepts are introduced.

2.1.1 Ferromagnets

A characteristic property of ferromagnets is that they acquire in comparison to paramagnets and diamagnets a very large magnetization in a relatively small magnetic field. This magnetization corresponds to the alignment of the atomic magnetic moments in the material. Many ferromagnets are saturated at fields much less than 1 Tesla. The value of the saturation magnetization varies with temperature, T, decreasing from a maximum value at $T = 0\,\mathrm{K}$ at first slowly, then more and more rapidly as T increases, becoming zero at the Curie temperature (T_{Curie} or in short T_{C}). Above this temperature it behaves like a paramagnet and the susceptibility follows the *Curie-Weiss law*:

$$\chi = \frac{C}{T - \theta}, \tag{2.1}$$

where C is a constant and θ is approximately equal to the Curie temperature.

So, it is stated that in the ferromagnetic materials, the magnetic moments have a strong tendency to align themselves with each other (this is due to the so called exchange interaction which is discussed below). However, when the applied field is removed, the magnetization can drop back to zero. Weiss, who studied this problem at the beginning of the 20th century, postulated the concept of magnetic domains because of this. This implies that a ferromagnet is divided into regions (domains), within which the magnetization is equal to the saturation value. Because of the different orientation of the magnetization in the different domains, the overall magnetization could be small or even zero. Saturation is produced by aligning the magnetization of each domain with the applied field.

The exact behavior of ferromagnets is described by the molecular field approximation, another concept introduced by Weiss. The details of this theory can be found in any book that treats magnetism, e.g., [1], [3] or [4].

A result of this theory is the temperature dependence of the saturation magnetization of a ferromagnet. That behavior is shown in figure 2.1.

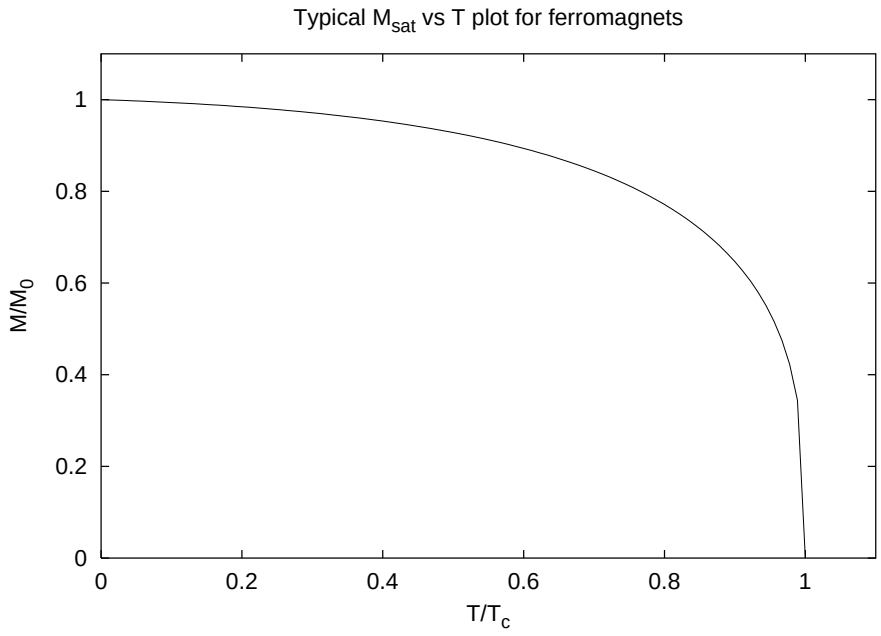

Figure 2.1: A typical plot of the behavior of the saturation magnetization as function of temperature for ferromagnets when no magnetic field is applied.

2.1.2 Important properties

Most magnetic materials show hysteresis when a field is applied. The variation of the magnetization M in a typical case is illustrated schematically in figure 2.2. Starting from the origin, it increases until it is saturated. The saturation magnetization is M_s, as is discussed in the previous section. When the external field H is now decreased, M does not decrease back to zero magnetization, but decreases in a much slower way. This results in a remanent magnetization M_r when the field has been brought back to zero. When the sign of the field is then reversed and the field is increased in strength again, at some point the magnetization will be zero again. The field needed to accomplish this is called the *coercive field* H_c. When the field is increased even further, the specimen will also reach saturation in the opposite direction. If the field is then decreased again and after that increased again to the maximum positive value, a loop is formed. This is called a hysteresis loop. The reason of this behavior is explained in detail in [3], for example.

The shape of the loop tells a lot about the material that is studied. The mentioned properties like M_r, H_c and M_s are very important if one wants to use the material for practical applications like permanent storage, electric motors (high H_c and M_r), or erasable recording (medium H_c, medium/high $M_\mathrm{s} = M_\mathrm{r}$).

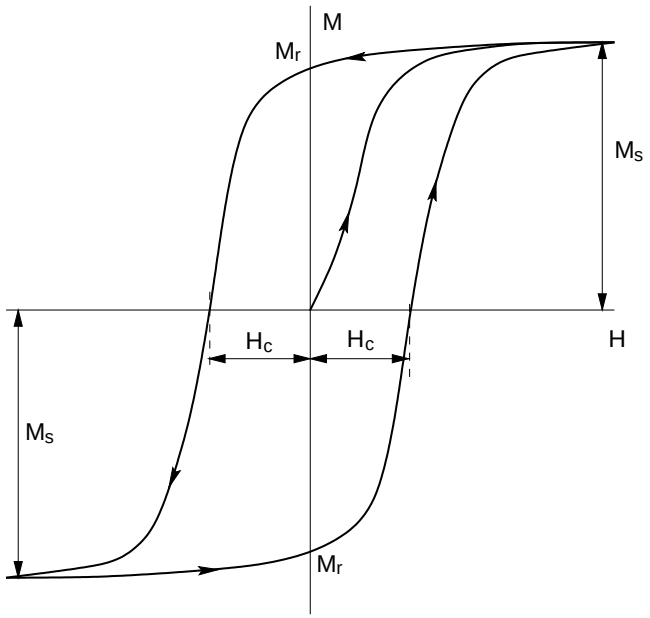

Figure 2.2: Variation of the magnetization of a typical magnetic material with applied field. See text for discussion.

2.2 Magnetic domain theory

This section introduces and explains some aspects of magnetic domain theory. For a more thorough discussion, see [3], for example.

As is discussed in the previous section, in 'normal' circumstances, magnetic materials are subdivided into domains, in which the magnetization is uniform and equal to the saturation magnetization M_s. However, the direction of the magnetization in those domains is different for different domains. The result is that the net magnetization is less than M_s. The reason why a magnetic material is in general not uniformly magnetized (single domain state), is that a material always wants to be in a state in which its energy is a minimum. So, it is useful to look at the energies and other phenomena that play a role in magnetic materials, which determine its state.

2.2.1 Exchange energy

The exchange energy can only be explained well in quantum mechanical terms. The exchange is really a result of the mixing of the two wave functions of neighboring atoms. Quantummechanically the exchange energy of the magnetic moments of two adjacent atoms i and j can be expressed in the form (see [5], for example)

$$w_{ij} = -2JS^2 \cos\theta_{ij} \tag{2.2}$$

where J is the exchange integral and S the total spin quantum number of each atom. So for $J > 0$ the lowest energy is attained when the spins are parallel to each other.

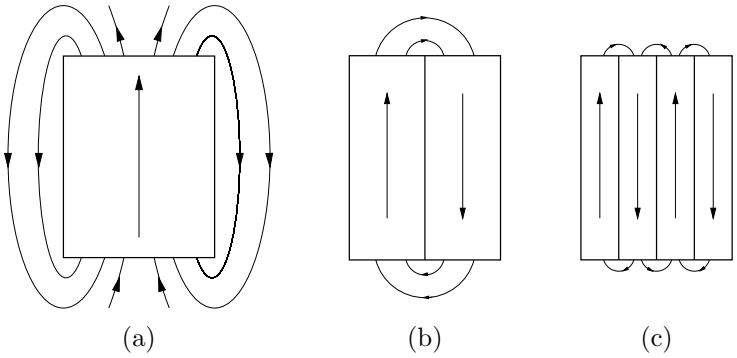

Figure 2.3: The stray field of (a) a uniformly magnetized specimen, (b) a specimen divided into two domains, and (c) one divided into four domains.

2.2.2 Demagnetizing energy

There is a second type of energy involved, which is large when the material is uniformly magnetized. Such a material would generate a large amount of stray magnetic field H, of which the energy can be expressed as

$$W_d = \frac{1}{2} \int H^2 dV, \tag{2.3}$$

where the integral must be taken over all space. This means that this energy is indeed smaller when the stray field is smaller. This is the case when the material is subdivided into more than one domain. See figure 2.3.

Another way of looking at this, is the following. In the example of figure 2.3(a), there will be a big magnetic north pole at the top of the specimen and a magnetic south pole at the bottom. The magnetic field lines always go from north to south, which means that *inside* the specimen the field is opposite to the magnetization. This is in fact the reason why the field inside the specimen is called the demagnetizing field. In figure 2.3(b) the top surface has both a north (on the left) and a south pole (on the right). In this configuration the demagnetizing field is much smaller, it is confined to the region near the two ends of the specimen. Now the demagnetizing field only tries to turn the magnetization in that region. If the specimen is subdivided into even more domains, the effect of the demagnetizing field becomes even smaller.

2.2.3 Anisotropy energy

The third kind of energy that we must take into account is the anisotropy energy, which arises from the crystalline nature of most magnetic materials. Simply said: it is easier to magnetize a material in certain directions. So the anisotropy energy depends on the direction of magnetization relative to the crystal lattice. The direction in which this energy is lowest is called the *easy axis*, since the material is easiest magnetized in that direction.

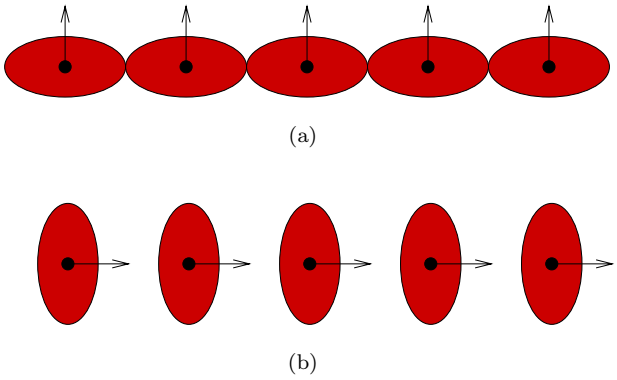

Figure 2.4: The asymmetry of the overlap of electron distributions on neighboring ions is one mechanism of anisotropy. The non-spherical charge distribution is caused by spin-orbit interaction, which ties the asymmetry to the direction of magnetization, so changing the spin direction changes the overlap energy (from [4], page 491).

An illustration of one origin of anisotropy is figure 2.4. The spin influences the orbital motion via the spin orbit interaction and in turn the orbital motion interacts with the crystal structure by means of the electrostatic fields and overlapping wave functions associated with neighboring atoms in the lattice.

Considering this energy the most important parameter is K_u, the uniaxial anisotropy constant. It is defined as follows:

$$E_a = K_u \sin^2 \alpha, \tag{2.4}$$

in which E_a is the anisotropy energy and α is the angle of the applied field compared to the uniaxial direction. So K_u is the proportionality factor between the anisotropy energy and the sine-squared of that angle.

2.2.4 Domain walls

The domain wall is the area between two oppositely magnetized domains. In that area, the spin direction varies smoothly from one state to the other. With the help of expressions of the exchange energy per unit area and the anisotropy energy per unit area of the wall, the following expressions can be derived:

$$w_{\text{wall}} = \pi \sqrt{\frac{A}{K}}, \tag{2.5}$$

for the domain wall width, and

$$\gamma = 2\pi \sqrt{AK}, \tag{2.6}$$

for the domain wall energy, in which A is the exchange constant and K the anisotropy constant in both formulae.

Note that there is always the balance between the exchange energy and anisotropy energy on the one side, and the demagnetizing energy on the other side, which decides whether the formation of a domain wall is favorable.

2.2.5 Magnetostriction

A last phenomenon that plays a role in the shape of magnetic domains is called magnetostriction. It is the effect that the shape of a specimen changes when its magnetization changes. Materials with a positive magnetostriction expand in the direction of magnetization and those with a negative magnetostriction contract. The effect also works the other way around: if a tensile stress is applied to a material with positive magnetostriction, it will be easier to magnetize it parallel and harder to magnetize it perpendicular to the axis of the tension, whereas if a compressive stress is applied, it will be harder to magnetize it parallel to the axis of compression. When the magnetostriction is negative, the opposite effect is observed. Effectively, the material acquires an extra contribution to the anisotropy, induced by the stress.

2.3 Ferrimagnetism

Ferrimagnetism plays a key role in the physics behind MO recording and read out. The materials used for the MO effect are amorphous alloys of rare earth (RE) and transition metal (TM) elements. Most of these alloys are ferrimagnetic, which means the magnetization of the TM sublattice is antiparallel to that of the RE sublattice. The net magnetization for the material is thus the vector sum of the individual magnetizations of the sublattices.

For some typical materials used for MO recording (like GdFeCo, TbFeCo) the general shape of the curves for the magnetization of the sublattices (M_{TM} and M_{RE}) and the net-magnetization M_s as a function of temperature are depicted in figure 2.5. The coupling (see 2.2.1) between the sublattices is responsible for the fact that the Curie-temperature for both is the same. At low temperatures, the magnetic moment of the RE component is bigger than that of the TM component. When the temperature increases, the magnetic moment of the RE component decreases faster than that of the TM component, which causes the net magnetic moment to decrease. At a certain temperature T_{comp}, the compensation temperature, the magnetic moments of the TM and RE component are identical but opposite, yielding a zero net magnetic moment. So, after this point there is an *increase* in the net magnetic moment until the magnetic moments of the sublattices start converging. In the end at the Curie temperature both magnetic moments vanish, so also the net magnetic moment. Beyond that temperature, the material is in a paramagnetic state.

Because of the different sublattices, we have to make a distinction between the measured Kerr-rotation (see section 2.6.1 for an explanation of this) angle and the actual magnetization of those sublattices.

If the electronic structure of both elements is looked at in detail, it is seen that the magnetic electrons of the TM are in the 3d electronic shell. This shell forms the outer layer of the ion, after the 4s electrons have been stripped off to the conduction band. On the other hand, the electrons responsible for magnetization of the RE elements are in the 4f shell, surrounded by the 5s, 5p and 5d shells, even after the outer 6s electrons are stripped off. The 4f electrons are laying so deep in the electron shell, that a lower energy photon (visible or infra red) will not have enough energy to interact with the magnetic electrons of the RE material, while it can easily probe the magnetic electrons of the TM

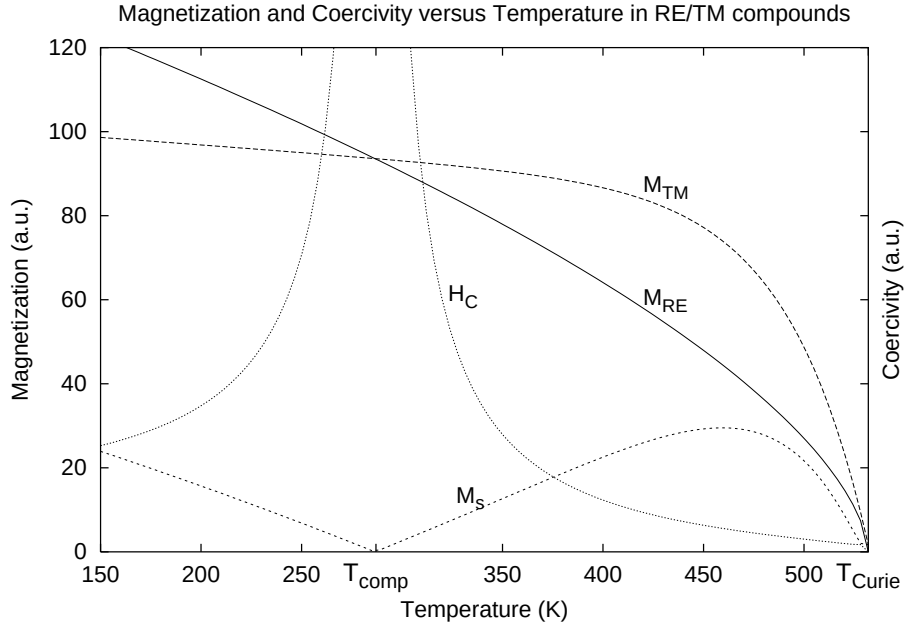

Figure 2.5: General behavior of the absolute magnetization and the coercivity (H_c) of the RE sublattice (M_{RE}) and the TM sublattice (M_{TM}) with temperature. The net magnetization of both sublattices is opposite and decreases in a different way with temperature. This means at a certain point (T_{comp}) they cancel and in the end they both vanish at the Curie temperature. The coercivity shows a great peak around T_{comp}, where it is infinite.

sublattice.

The electronic structure of the RE and TM is such, that the RE component is in general not sensitive for visible light, i.e., $\lambda > 400\,\text{nm}$, which means that a laser probe in this wavelength regime will only experience Kerr-rotation due to the TM (see also [6]). This is shown in figure 2.6, where the wavelength dependence of the Kerr rotation is plotted. The rotation switches sign well below 300 nm, which indicates that there the RE component becomes more important than the TM component. So the net magnetization will be totally different from what the Kerr-rotation indicates. One can derive the net magnetization curve if the curves for both individual components are known.

A last remark about this kind of materials: the uniaxial anisotropy is directed along the surface normal and decreases approximately linearly to zero at T_{Curie} with increasing T.

2.3.1 Coercivity of a ferrimagnet

The coercivity of a ferrimagnet as a function of temperature is of course also an important relation. It can be derived with the help of the information in [7] and [8], for example.

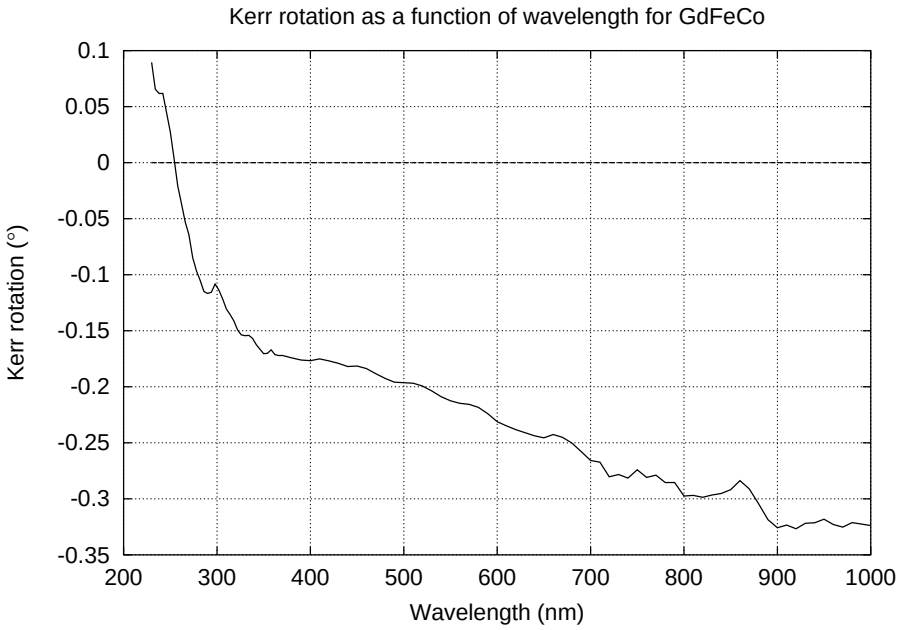

Figure 2.6: The wavelength dependence of the Kerr rotation of GdFeCo reveals that the RE component (giving 'positive' rotation angles) becomes important below 300 nm.

In general the anisotropy field (i.e., the maximum coercivity, the field needed to change the magnetization from easy to hard direction) of a material is given by

$$H_u = 2K_u/M_s. \tag{2.7}$$

For a ferrimagnetic specimen, M_s is just the difference between the magnetizations of the two antiparallel magnetized subnetworks:

$$M_s = |M_{\mathrm{TM}} - M_{\mathrm{RE}}|. \tag{2.8}$$

For the anisotropy we can write the following relation:

$$K_u = \frac{1}{2}\sum_{i\neq k} C_{ik} M_i M_k, \tag{2.9}$$

in which $i = 1$ refers to the rare-earth sublattice and $i = 2$ to the transition metal sublattice. The result is:

$$K_u \propto M_{\mathrm{RE}} M_{\mathrm{TM}}. \tag{2.10}$$

However, in [8] the anisotropy is given by

$$K_u = (|M_1| + |M_2|)^2, \tag{2.11}$$

which is of course the same as

$$K_u = M_1^2 + 2|M_1 M_2| + M_2^2. \tag{2.12}$$

The latter is just a little different from equation (2.10). For the coercivity, this means:

$$H_c(= H_u) \propto \frac{M_{\mathrm{RE}} M_{\mathrm{TM}}}{|M_{\mathrm{TM}} - M_{\mathrm{RE}}|}, \tag{2.13}$$

following [7]. When the expression from [8] is used, there are some extra M^2s in the numerator, creating only a vertical offset. This result means for instance that the coercivity of the ferrimagnetic material goes to infinity at T_{comp}. Around T_{comp} the coercivity changes drastically with temperature.

2.4 Domain reversal in general

In general, the magnetization can be changed (and thus also the domain structure) by applying an external magnetic field. This can be explained with the help of the equation for the energy added by the applied field per unit volume

$$E_H = -\vec{M} \cdot \vec{H}. \tag{2.14}$$

As can be seen from the dot product, the energy is a minimum when H and M are parallel and a maximum when they are antiparallel. In a specimen containing, say, two domains of opposite direction the effect of an applied external field is as follows. The energy for the two domains is different, since they both have another component in the direction of the magnetic field (unless they are both perpendicular to it). This energy can be reduced in two ways. Firstly, the domain wall can move, increasing the volume of the domain with the lower energy and decreasing the volume of the domain with the higher energy. Secondly, the magnetization direction of the domains can change. Those two mechanisms can occur simultaneously in practice.

The position of the domain walls depends on the demagnetizing energy. The externally applied field adds up to the demagnetizing field, generally moving the domains to new positions. Since the magnetization directions are mainly governed by the anisotropy, for small fields there will be only domain wall motion, and rotation will only occur for larger fields.

Generally, domain wall motion is only reversible for very small applied fields. Normally the walls do not return to their begin position when the applied field is removed. This is because of the inhomogeneities in the sample. The domain walls will move until a force on the wall can stop it. A local inhomogeneity that stops the movement of domain walls is called a pinning site. At those defects the exchange and anisotropy is a lot lower, resulting in pinning of domain walls.

2.5 Reversal dynamics: Bloch equation

To explain the dynamics of thermo-magnetic writing as is measured in section 3.2.2, an adapted version of the Bloch equation is used. The normal Bloch equation describes barrierless magnetization reversal due to an oppositely directed external field at constant temperature T, so that the final magnetization is constant (M_0):

$$\frac{dM(t)}{dt} = \frac{-M_0 - M(t)}{\tau}, \tag{2.15}$$

with the solution (cf. figure 2.7 (c))

$$M(t) = -M_0 + 2M_0 e^{(-t/\tau)} \qquad (M(0) = M_0). \tag{2.16}$$

From this equation it is obvious that τ is a characteristic time for the asymptotic magnetization reversal and therefore generally called the reversal time. Note that in [9] it is shown that this equation can also be used to describe reversal by transient domain formation.[1]

However, for thermo-magnetic writing clearly the situation is different: the temperature is not constant. Therefore M_0 has to be replaced by $M_0(T(t))$, the temperature induced magnetization dynamics (i.e., the changes in the saturation magnetization caused by the changes in temperature). This is justified when $M_0(T(t))$ is related to $T(t)$ via the equilibrium magnetization curve.

The resulting modified Bloch equation is

$$\frac{dM(t)}{dt} = \frac{-M_0(T(t)) - M(t)}{\tau}. \tag{2.17}$$

The so called reversal time τ, denoting the material specific response time of M to magnetic fields, can only be measured at a fixed temperature actually (cf. figure 2.7 (c), where τ is just the $1/e$ value of the solution of the normal Bloch equation (equation 2.15)). However, the dynamics of thermo-magnetic writing depend on τ and $M_0(T(t))$, i.e., the cooling rate. So in this case τ corresponds to the delay between the recovery and reversal of M.

A simulation was made to illustrate all this, see figure 2.7. The temperature was assumed to have the time evolution as is shown in figure 2.7(a). To calculate the magnetization dynamics due to this transient temperature, the following formula was used:

$$M_0(T) = M_{(T=0\,\mathrm{K})}(1 - \frac{T}{T_\mathrm{C}})^{exp} \tag{2.18}$$

in which the critical exponent exp was 0.66 and $T_\mathrm{C} = 530\,\mathrm{K}$ in the simulation. This resulted in a magnetization recovery curve as is shown in figure 2.7(b). Figure 2.7(c) shows the solution of the normal Bloch equation as is stated above and (d) shows the resulting solution of the adapted Bloch equation (2.17), which can only be calculated numerically. In (e) the magnetization dynamics shown in (b) has been inverted and plotted together with the curve of (d). This shows that there is indeed a delay between the recovery and reversal of M. In (f) it is shown that this delay is equal to τ: when the switching curve is shifted τ to the left, the curves (almost) overlap. This overlap will be less and less accurate when τ gets in the same time regime as the cooling time.

Note that the Landau-Lifshitz-Gilbert equation, widely used to describe the magnetic response to field pulses, predicts no response for anti-parallel orientation of M and H_ext. It only describes what happens if there is a moment on the spins, caused by H. But when H and H_ext are antiparallel ($\vec{H} \cdot \vec{M} = 0$), this equation is not appropriate.

[1] The formula for $M(t)$ as is given in that paper (on page 4879), is just the solution of the Bloch equation, except for the λ/λ_s factors. Those are not important for our case though: we use high fields and there is no field dependence in the time regime of our experiment, meaning $\lambda = \lambda_s$.

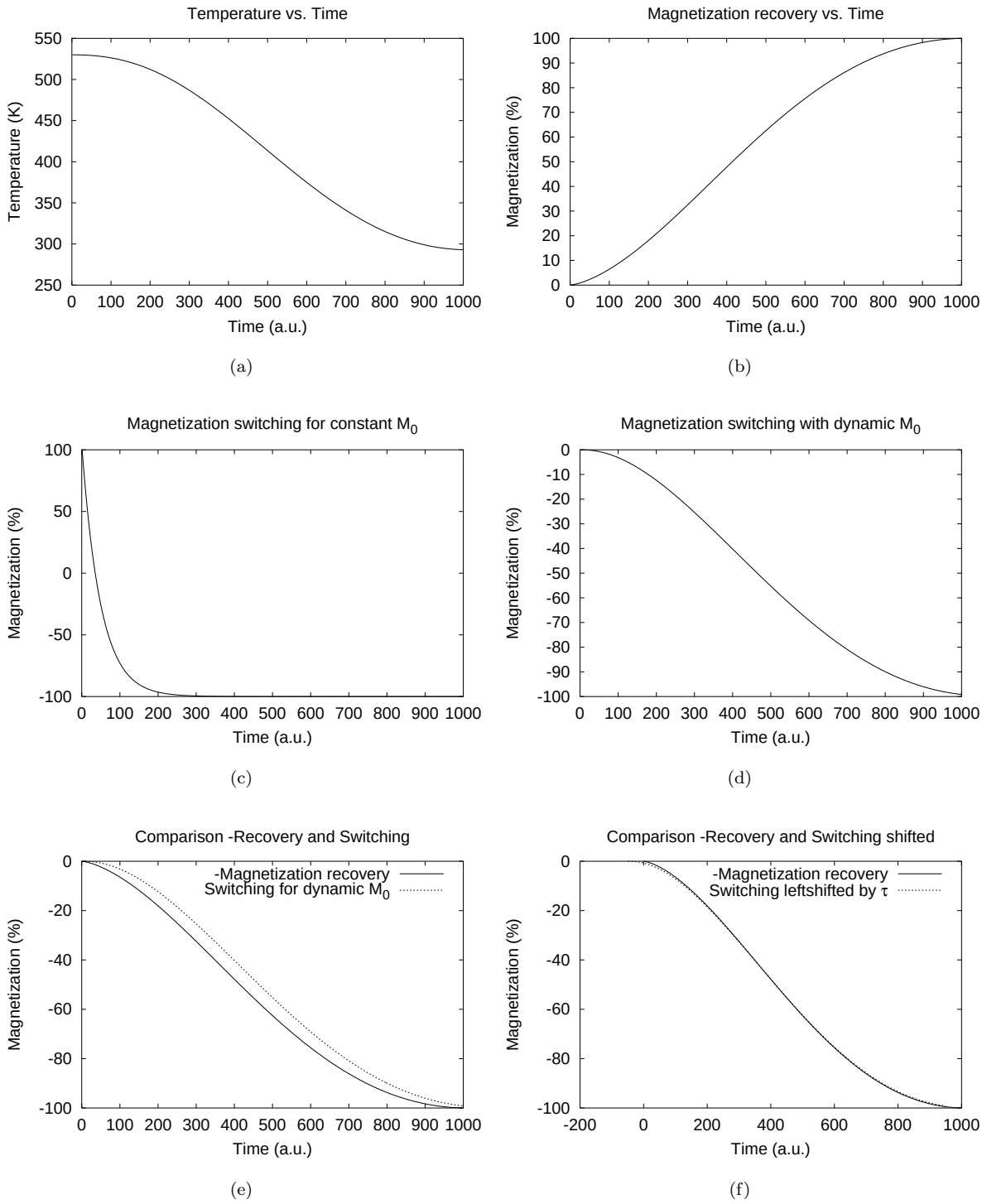

Figure 2.7: Illustration of the difference between the normal and the adapted Bloch equation. (a) shows the used transient temperature and (b) the resulting magnetization dynamics via the equilibrium magnetization curve. In (c) the reversal process for the normal Bloch equation is shown, while (d) shows what happens for the adapted version. In (e) the curve of (b) is inverted and compared to the curve of (d). When the curve of (d) is shifted over a time τ to the left, they almost overlap (f). So τ represents the delay between the recovery and reversal of M.

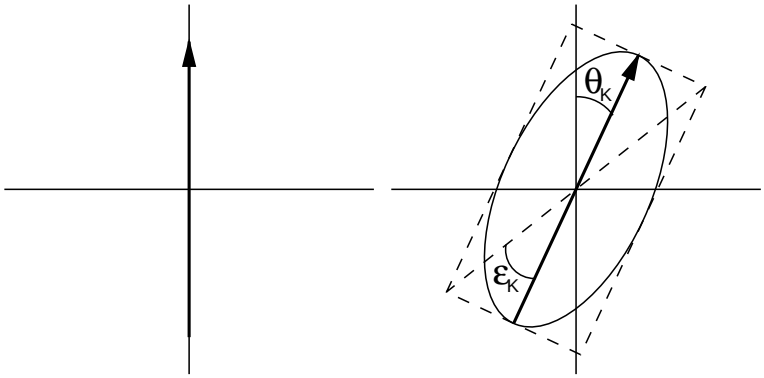

Figure 2.8: The magneto-optical Kerr effect changes the incident plane polarized light (a) into elliptically polarized light (b). The direction of polarization is also changed by the angle θ_K. The ellipticity is defined as the angle ϵ_K, as shown in the figure.

2.6 MO systems

As has been discussed in the introduction, the first generation MO systems used the Magneto Optical Kerr Effect (MOKE) to read out the data. This effect plays a central role in the experiments that have been done and in all MO systems. Therefore it is explained here also, following the treatment in [10], chapter 3.1 and [11] (e.g., pages 41 and 42).

2.6.1 The Magneto-Optical Kerr Effect

The effect that when plane polarized light is reflected from a surface of a magnetized object the polarization is changed depending on the magnetization of the material is called the Magneto-Optical Kerr Effect (MOKE). In the general case, the reflected light is not plane polarized anymore, but has become elliptical, see figure 2.8. The origin of the effect lies in different coefficients of refraction for left- and right-handed circularly polarized light, which are both equally present in linearly polarized light. The quantitative description of this is as follows.

If we consider that the surface of a crystal with cubic symmetry is illuminated at normal incidence, we can write for the dielectric tensor ε

$$\varepsilon = \begin{pmatrix} \varepsilon_0 & \varepsilon_1 & 0 \\ -\varepsilon_1 & \varepsilon_0 & 0 \\ 0 & 0 & \varepsilon_0 \end{pmatrix}, \tag{2.19}$$

expressed in terms of the Cartesian x and y polarizations of the cubic crystal. Note that only the elements for the polar Kerr effect[2] have been taken into

[2]meaning that the magnetization is perpendicular to the surface on which the light reflects.

account. This tensor is related to the index of refraction n by

$$n^2 = \varepsilon. \tag{2.20}$$

If those two equations are combined, the following eigenvalue equation is acquired:

$$\begin{vmatrix} \varepsilon_0 - n^2 & \varepsilon_1 & 0 \\ -\varepsilon_1 & \varepsilon_0 - n^2 & 0 \\ 0 & 0 & \varepsilon_0 \end{vmatrix} = 0, \tag{2.21}$$

where the zz element is left as it was, since the polarization does not have a z-component. The solution of this equation yields the eigenvalues

$$n^{\pm} = \sqrt{\varepsilon_0 \pm i\varepsilon_1} \tag{2.22}$$

with the corresponding eigenvectors

$$E^{\pm}(\omega) = E^{\pm} e^{i\omega(t - 1/cn^{\pm}r)}, \tag{2.23}$$

which describe circularly right- (for the pluses) and left-handed (for the minuses) polarized light.

To express the Kerr effect in the dielectric tensor elements ε_0 and ε_1, the polarization variable χ is used, which can be expressed as:

$$\chi = \frac{E^+}{E^-} = \frac{r^+}{r^-}, \tag{2.24}$$

where E and r are the polarization amplitudes and the coefficients of reflection respectively, for the two directions of circular polarization. The Kerr effect can be expressed by the complex Kerr angle $\Delta_K = \theta_K + i\epsilon_K$, of which the components are sketched in figure 2.8. With the help of (2.24), they can be calculated:

$$\chi = \frac{r^+}{r^-} = \frac{(n^+ - 1)/(n^+ + 1)}{(n^- - 1)/(n^- + 1)} = \frac{1 + \tan\epsilon_K}{1 - \tan\epsilon_K} e^{-2i\theta_K}. \tag{2.25}$$

If this equation is combined with (2.22) and one only considers small Kerr angles, it yields

$$\Delta_K = \theta_K + i\epsilon_K = \frac{\varepsilon_1}{\sqrt{\varepsilon_0}(1 - \varepsilon_0)}. \tag{2.26}$$

So, in the case of $\varepsilon_1 = 0$, i.e., in the case there are no off-diagonal elements in the dielectric tensor, there is no MOKE.

So the real origin of MOKE lies in the origin of the off-diagonal elements of the dielectric tensor. The origin of those elements can be quantummechanically explained with the concept of spin-orbit interaction. However, the precise derivation of them goes beyond the scope of this thesis. A very thorough explanation from several points of view can be found in the first chapter of [12].

2.6.2 MAMMOS

If the bit densities of the recording media get beyond what is optically resolvable, other methods of reading out should be developed. This is currently the issue in MO recording. It is possible to make magnetic domains much smaller than the

spot size of the readout laser beam. This means that the recorded bits cannot be individually read out.

The basic idea of MAMMOS is: use the heat profile of a laser beam to intensify the stray field of the recorded domains so that they are copied into an additional magnetic layer—the readout layer— of which the coercivity is decreased because of the rise in temperature. Then the copied domain is expanded with an external field up to the laser spot size to get a saturated MO signal level from the small recorded domain. Note that in practice those two steps happen at the same time: copying is helped by the external field and after that expansion follows immediately.

The above mentioned properties of ferrimagnetic materials are of crucial importance for the mechanism of MAMMOS. The recording layer, in which the bit pattern is stored, is made of the alloy TbFeCo, whereas the readout layer is made of GdFeCo. TbFeCo is in general a magnetically harder material than GdFeCo. This suits better to the storage layer. The composition is chosen such that the compensation temperature of the layers is roughly around 0°C. This means that the magnetization of the materials will *increase* with temperature (until a certain temperature after which it decreases again, see above). Also, the coercivity will decrease with temperature.

So, at room temperature the coercivity of the recording layer is very high, to prevent accidental erasure of the magnetic information. At this temperature the coupling between the two layers can be neglected, since the coercivity of the readout layer is high and the magnetization of the recording layer is low.

When the actual readout is happening, the readout laser beam is heating the MAMMOS disk. This means the magnetization of the recording layer will increase and the coercivity of the readout layer decreases. The temperature profile of the laser beam is chosen such that the region where the temperature is sufficiently high to enable copying is smaller than half the size of one bit domain. With this size it is ensured that at maximum one domain is copied and no interference of other domains occurs. Of course this region is much smaller than the spot size of the beam. This is illustrated in figure 2.9.

Thus, in this region the magnetic domain is copied to the readout layer. After copying of the domain an external field expands it when its direction is parallel to the magnetization of the domain. This happens because the external field changes the balance of energies in the copied domain in such way that it can grow. Usually the expanded domain becomes about as big as the laser spot. This means the domain can be easily read out. After readout, the direction of the external field is switched so that it shrinks the copied domain (if there was one) until it collapses. This brings the state of the read out layer back to its original configuration. So, an external field of square wave form is used to expand domains in case they are in the same direction as the field and to collapse them afterwards to get identical initial situations. Thus note that in case the magnetization of the copied domain is in this 'collapse' direction, no expansion will take place (since the expansion only occurs due to moving domain walls, and there are no domain walls in this case) and during readout the magnetization of this oppositely magnetized domain will indeed be read out. The complete cycle is schematically shown in figure 2.10, after [2].

This also means that in practice it is very complicated to time everything well: the period of the external magnetic field is directly related to the rotation speed of the disk and thus the size of the recorded domains.

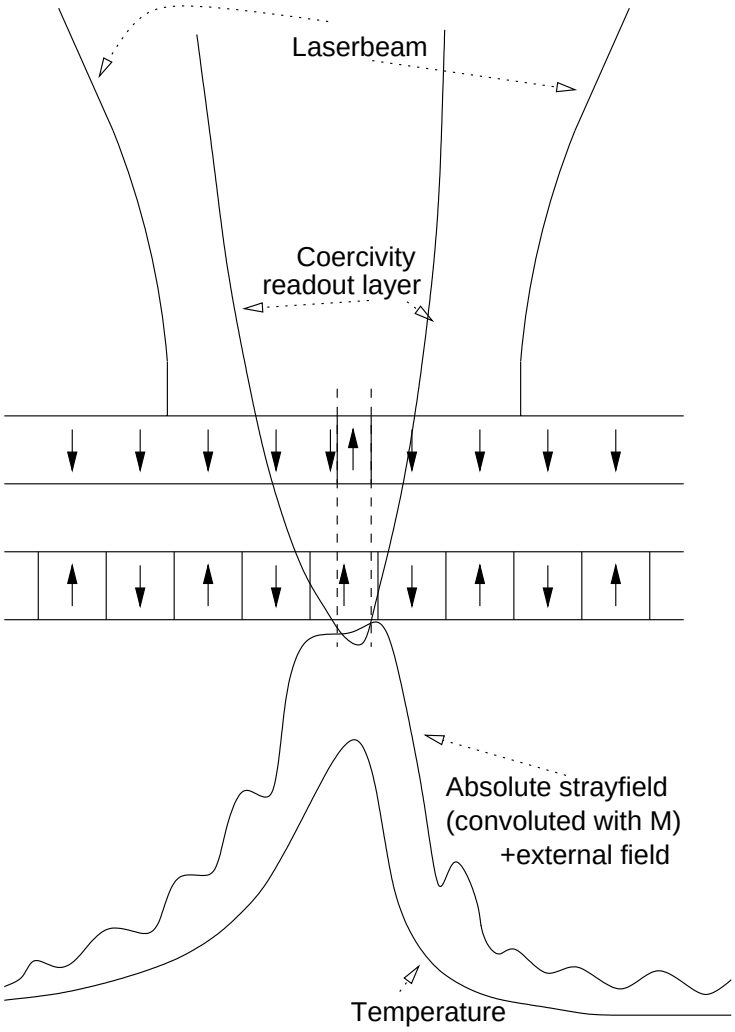

Figure 2.9: Schematical illustration of the mechanism of MAMMOS. The temperature profile allows a domain to nucleate in the read out layer. In practice, an external field helps to do this at lower laser powers. After this, the nucleated domain expands and can be read out (not depicted). Note that the net stray field is very much influenced by the edge effect of the domains (at domain boundaries a higher stray field occurs), hence the wobbly shape of that curve. The disk motion is to the left, in this figure.

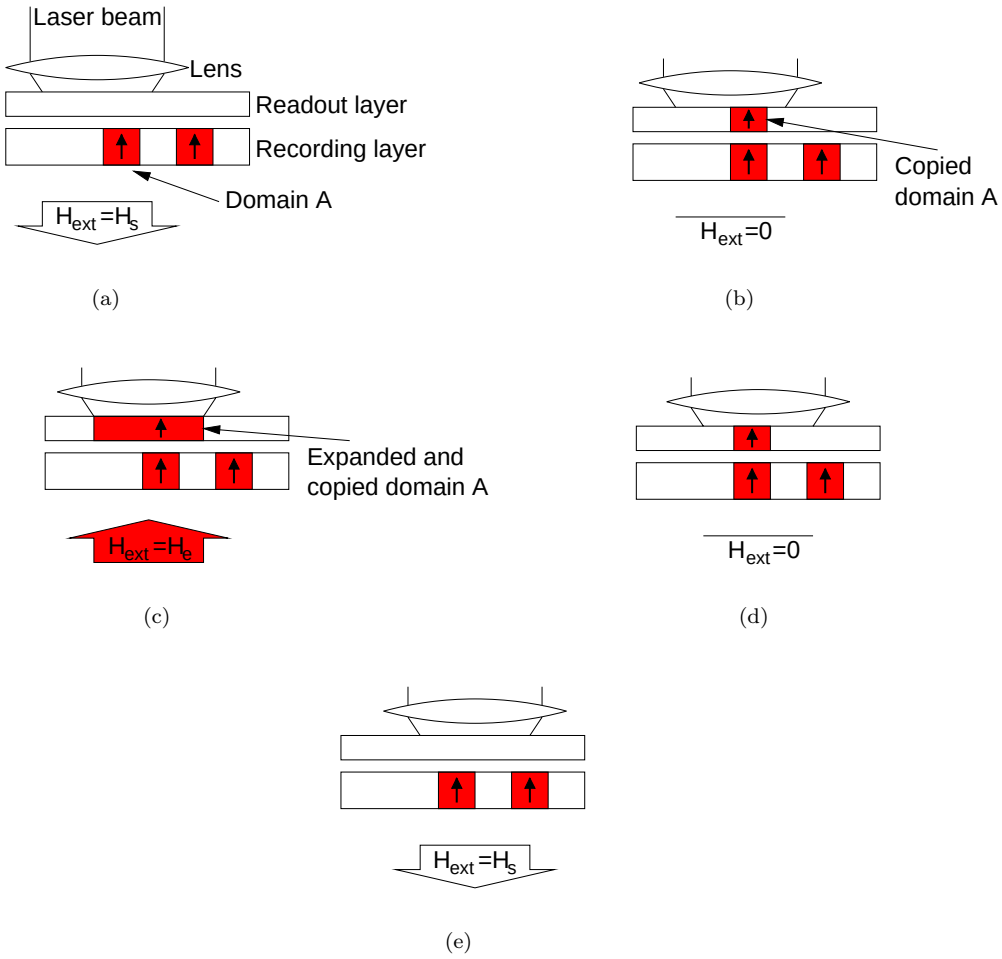

Figure 2.10: Flowchart of MAMMOS as is explained in the text.

Chapter 3

Experiments

3.1 CW MOKE measurements

To investigate the magnetical and magneto-optical properties of the readout layer, magnetic hysteresis loops were measured as a function of temperature using linear MOKE detection.

The measurements consist of making Kerr-hysteresis loops at different temperatures. From such loops, the following properties can be derived:

1. Kerr rotation as a function of temperature (and thus magnetization change with temperature of the RE- or TM-component of the GdFeCo, depending on the used wavelength),

2. coercivity as a function of temperature.

Those properties are obviously of vital importance for MAMMOS.

In this section the set up, sample and the results are discussed.

3.1.1 Set up

The set up for these measurements is depicted in figure 3.1. It is a standard MOKE set up. The idea is that the incoming polarized light undergoes a polarization rotation caused by the magnetized sample. The rotation direction depends on the magnetization direction, see also section 2.6.1. To make hysteresis loops using this effect, the material is first magnetized in one arbitrary direction. Then, the analyzer is set such, that the outcoming signal is as close to zero as possible (i.e., the analyzer and polarizer are cross-polarized and the rotation caused by the current magnetization of the material has been compensated). Any change in magnetization (and thus rotation) will have a huge effect on the transmitted light intensity, which is proportional to the rotation angle and the magnetization itself. This is illustrated (without the compensation) in figure 3.2. To improve the signal to noise ratio, a modulation technique was used. A Faraday cell modulated the signal and its frequency was used as reference for a lock in amplifier.

The disadvantage of this set up is that it is sensitive for changes in the intensity of the laser beam. However, the acquired signal was so large, that there was no noticeable influence of this.

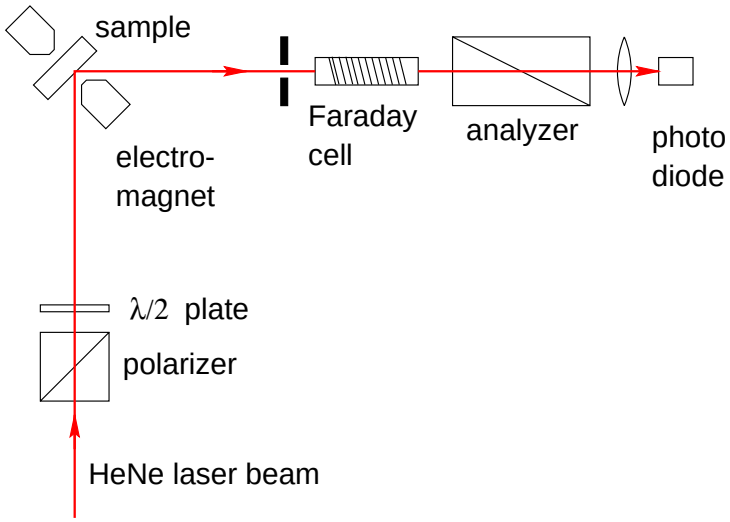

Figure 3.1: The setup that was used for the MOKE experiments. The s-polarized light from the HeNe laser goes through a polarizer in s-direction to filter out any non-s components. It is then converted to p-polarized light with the $\lambda/2$-plate (note that it is also possible to use just s-polarized light, it makes no difference in this case). After the plate, the light is reflected on the sample, passes the Faraday cell which is used for modulation and goes through the analyzer. The resulting light is focused on the photo diode, which is connected to a lock-in amplifier having the signal on the Faraday cell as reference. Note that in general it is better to put the modulator in the beam before it interacts with the sample, but in this case there was no noticeable difference.

The current through the coils of the electromagnet was automatically regulated. The magnetic field was always actually measured during the measurement, so that no errors could occur due to a bad calibration of the I versus B curve of the magnet nor because of remanence in the magnet poles.

An additional parameter that was important to investigate was temperature. Therefore a heating stage was prepared. This stage merely consisted of a piece of aluminum with a clamping mechanism to keep the sample on it. The piece of aluminum has holes in it through which a filament wire is run. So by running a current through the wire, the piece of aluminum heats up and in this way the temperature of the sample can be increased. To monitor the temperature, a Pt-100 thermo-resistor is placed just below the sample.

There is an issue whether this is an accurate way of controlling the temperature with this simple set up. The most important factor will be the large diffusion (cooling) to the air at the sample surface. Also, the temperature is measured *under* the sample and the measurements are taken on the sample surface. There was not much that could be done about this. One way of improving this may be to put a box around it, but that will not help so much: it will only decrease the cooling by air flow, so the diffusion to air will be less effec-

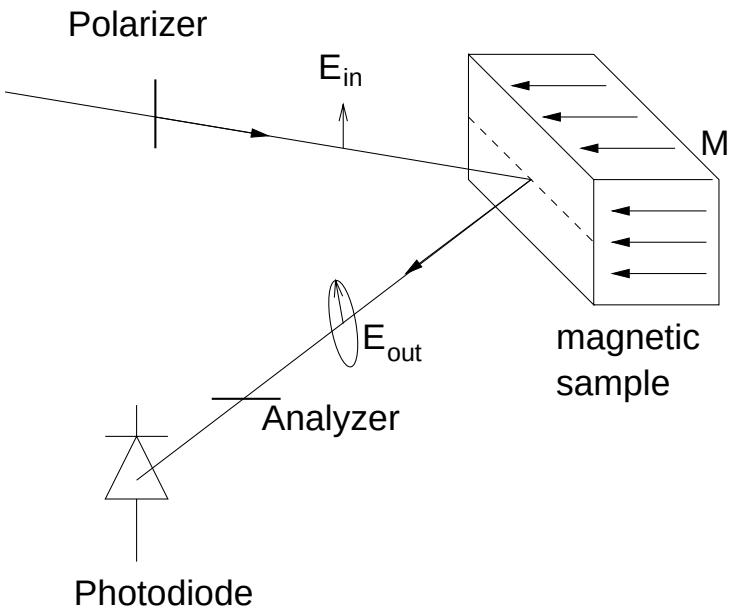

Figure 3.2: The simplest way to detect changes in magnetization using MOKE. The change in rotation due to the magnetization of the sample will result in changes in the intensity of the light beam on the photo diode. This principle was used in the set up.

tive. However, when the temperature was changed quickly (by blowing, e.g.), the result was immediately visible in the temperature signal, which indicates only a small lag in the temperature read out. The temperature sensor itself was quite accurate. Although only two wires were used, it is still accurate within one degree.

So, with this setup hysteresis loops as a function of the temperature can be recorded.

3.1.2 Sample

All preliminary measurements were done on a sample named AZA161#7. This sample consists only of a MAMMOS readout layer. The sample structure is depicted in figure 3.3.

This sample, made by magnetron sputtering on glass, consists of the following components. An AlTi layer, which serves as a heat sink and reflectivity enhancer. On top of that is a thin layer of SiN, on which the active MO layer, made of $Gd_{23.1}Fe_{71.9}Co_{5.0}$ is sputtered. The top layer is again made of SiN. It is a protective layer and the thickness is tuned for optimum transmittance for a certain wavelength, in this case 680 nm. Note: for MAMMOS this is not the optimum wavelength for the MO signal, but for this wavelength the tracking and focusing works better. So this thickness is suitable for a relatively good MO signal and servo signals.

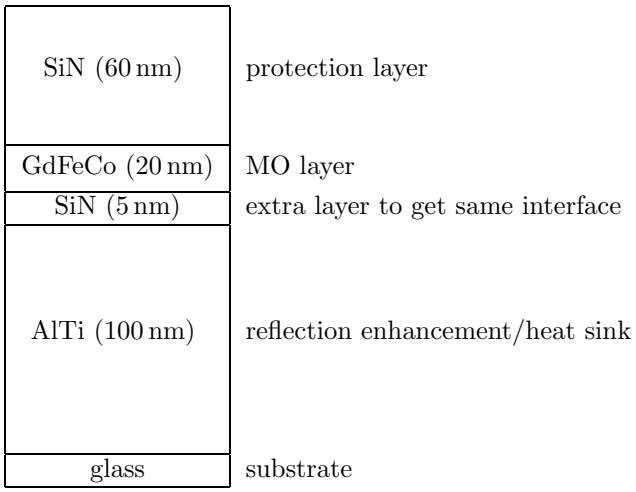

Figure 3.3: The structure of sample AZA161#7. On the left the materials and thicknesses are indicated and on the right their function is mentioned.

3.1.3 Results

The resulting Kerr-hysteresis loops are shown in figure 3.4. At room temperature the loops are very square with $H_c > 300$ Gauss (so it is quite stable), which was expected for a MO recording material. Also as expected, the loops get narrower when the temperature increases (which means that the coercivity decreases) and the total Kerr-rotation decreases also with increasing temperature, as only the TM component is probed.

Because in the above mentioned figure it is not clear what happens at higher temperatures, a zoomed in graph is shown in figure 3.5, in which only the loops at the highest temperatures are shown. From this graph it can be seen that the hysteresis loops tend to get less square than normal, and when the temperature reaches T_C, the coercivity becomes really zero, although the magnetization is still not exactly zero. This is because of the fact that above T_C, the ferrimagnet becomes a paramagnet, showing magnetization proportional to the applied field.

After those measurements, the sample was cooled down. Also during this procedure some hysteresis loops were recorded. They are displayed in figure 3.6. Striking is the asymmetry in the loops. The left wing of the loop is not 'square' anymore, although the right part is. The exact reason for this is not known. It might have to do something with diffusion of oxidized N-atoms to the MO-layer. Also, the coercivity has decreased tremendously (and the total magnetization too, a little), which means the measurements had a big annealing effect causing structural relaxation or even crystallization: the amorphous structure of the material changed under influence of the higher temperatures. This has a big influence on the anisotropy of the sample, which originates in stresses in the material. It was observed in other measurements that for very long and extensive heating the anisotropy turned even in plane.

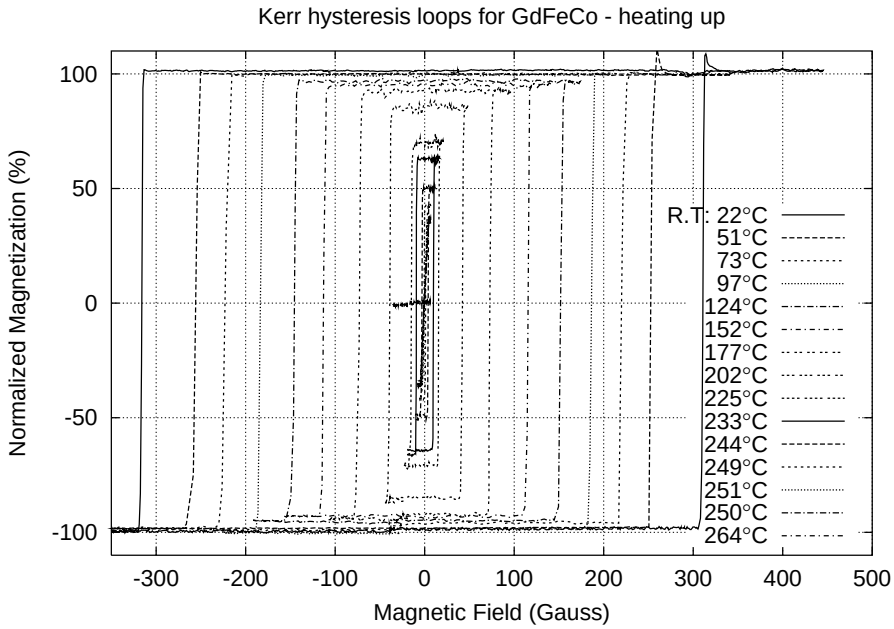

Figure 3.4: Kerr-hysteresis loops for a fresh GdFeCo sample as described above, for different temperatures.

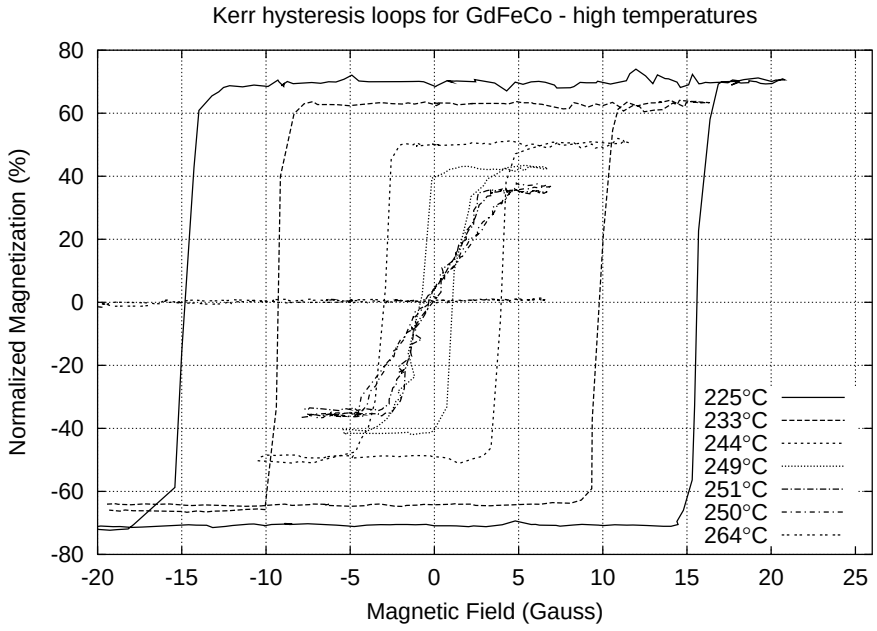

Figure 3.5: Zoom in on the higher temperatures.

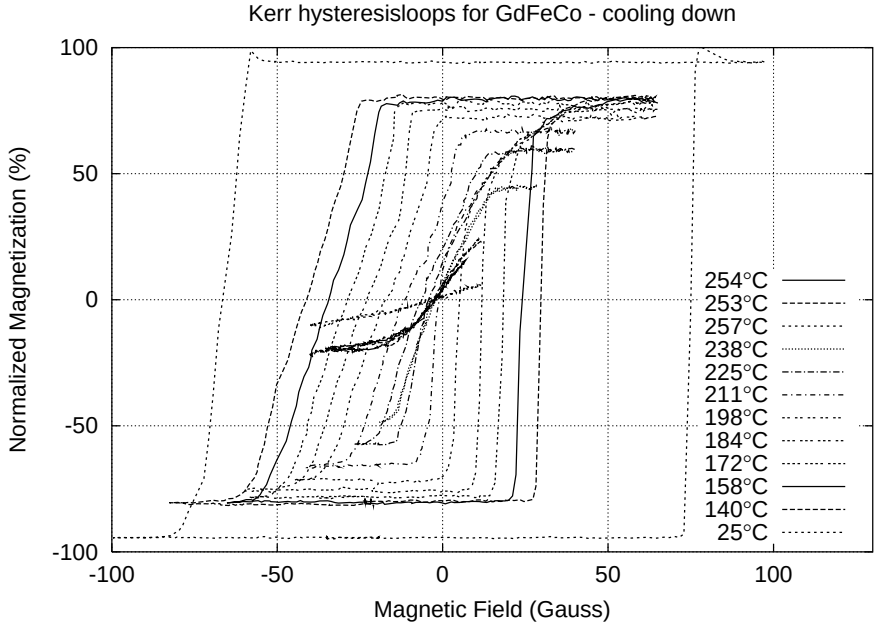

Figure 3.6: Kerr-hysteresis loops when cooling down the sample. See the text for discussion.

3.1.4 Magnetization dependence on T for GdFeCo

If the analyzer and polarizer are exactly cross polarized, no light will reach the diode, meaning zero signal. If then the magnetization is switched, we have the maximum signal. If then the analyzer is turned to cross-polarized condition again, the total rotation angle is found by looking at the angle the analyzer had to be rotated to get zero signal again. This was done during the measurements with the hysteresis loops. The total rotation as a function of temperature is shown in figure 3.7. It is proportional to the magnetization of the TM compound of the GdFeCo, since the wavelength of the HeNe laser is 632.8 nm.

In the figure two datasets are plotted. The first one is from data with a temperature range up to 200°C. For these data points a curve could be fitted of the form

$$M = M_0(1 - \frac{T}{T_\mathrm{C}})^{exp}, \tag{3.1}$$

in which *exp* is a critical exponent. With the fit made to the first dataset, the Curie temperature could be extrapolated. The result was $T_\mathrm{C} = 235°\mathrm{C}$. However, the second dataset is for the same sample. The history of this sample was a little different (it had had several heat treatments from previous measurements), resulting in an almost completely different curve. This time the above mentioned curve could not be well fitted to the data. The attempt is shown in the figure. The resulting Curie temperature was $T_\mathrm{C} = 245°\mathrm{C}$.

This effect is not a matter of inaccurate temperature measurements. For a discussion about this accuracy, see above. However, it must be noted that during these measurements the sample undergoes some serious changes. Especially

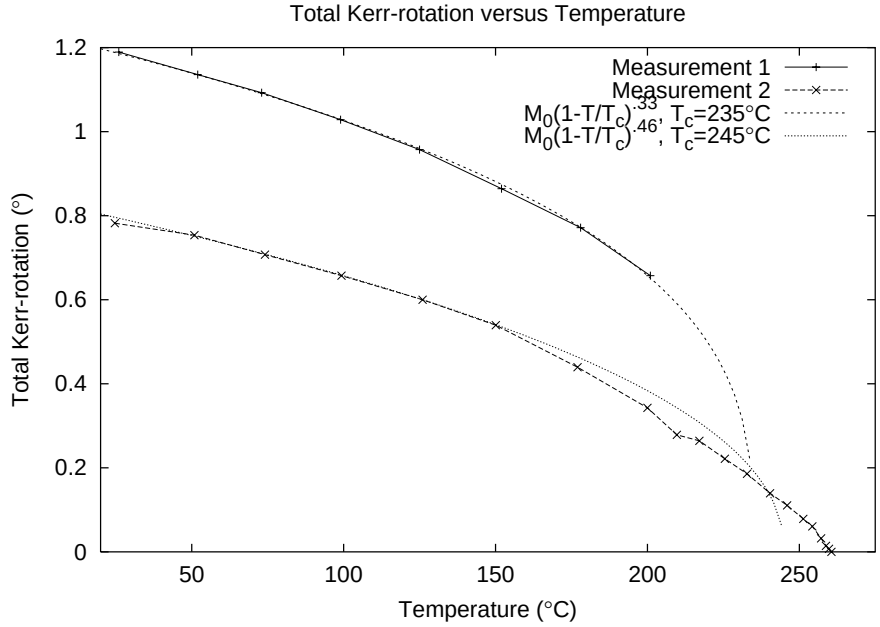

Figure 3.7: Total Kerr rotation (and thus magnetization of the TM component) as a function of temperature for two different measurements on the same sample. See the text for discussion.

when measuring for a long time at high temperatures, structural relaxation takes place and maybe even some crystallization. That is why the Curie temperature cannot be accurately determined by this kind of measurements. The data points for higher temperatures are probably not correct, under influence of the changes in the material at that temperature. Also, under the heat treatment, the position of the compensation temperature may change, as it is very drastically dependent on the exact composition of the material. If this happens, the magnetization can be different and thus the amount of rotation. In a practical MAMMOS system this effect can be neglected, since the short laser pulses put a lot less energy into the sample. There have been done some tests regarding this, but as expected there was not an important influence.

3.1.5 Coercivity as a function of T for GdFeCo

In figure 3.8 the coercivity as a function of temperature is plotted, as extracted from figure 3.4. The shape of this curve appears to be about linear. One would expect an exponential decay (as in figure 2.5), but that does not seem to happen. Maybe the compensation temperature of this sample is somewhat lower than expected, so that this part of the curve turns out to be about linear.

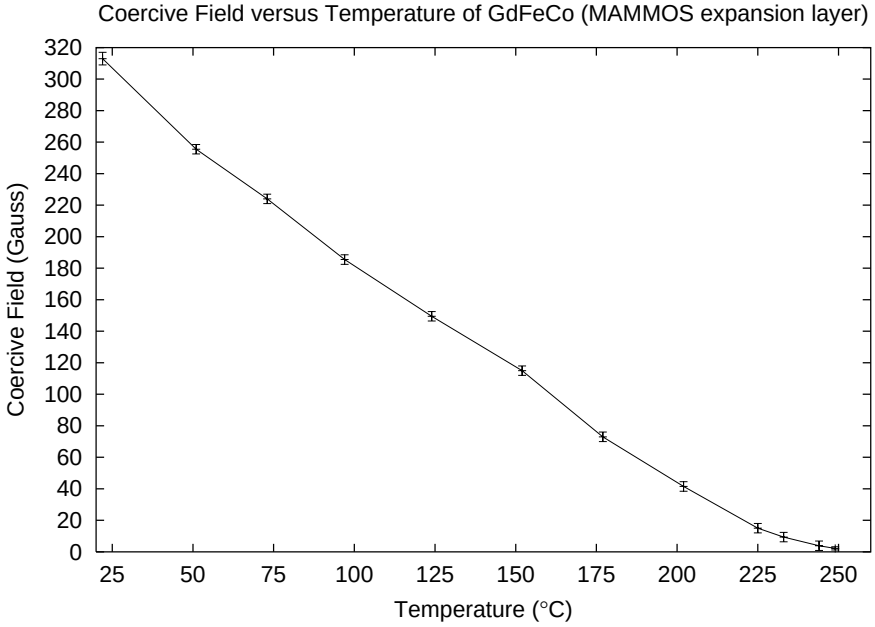

Figure 3.8: Extracted coercivities from the Kerr hysteresis loops of a fresh sample.

3.1.6 Temperature dependent hysteresis loops in a MAMMOS sample

To get a more complete picture of what happens with the hysteresis loop of an initialized MAMMOS sample as a function of temperature, we have also done some measurements on such a sample. The motivation for this is the unexpected results obtained when looking at its domain structure when heating it, see section 3.3.4.

At room temperature, the measured sample (AZG111#7, again, see below) shows a normal 'square' hysteresis loop. But as the temperature increases, the loops start to deform in two ways. The first thing is that the total magnetization decreases, which is expected, since this should be the case in any MAMMOS sample. But a second effect is that the loop gradually splits up in two sub loops, see figure 3.9, which looks like some sort of double layer switching behavior: the two layers being parallel (large M) at large fields and anti-parallel (small M) at small fields. The total width of the curve increases and the width of the sub loop decreases with increasing temperature. At about 220°C the width of the sub loops is so small, there is no hysteresis anymore.

When cooling down, a very similar behavior is found. See figure 3.10. The loops at the highest temperature are virtually identical to the ones obtained when heating up. The loops at the lower temperatures look similar. However, when studied more carefully, it can be seen that the curves are more deformed in the cooling down series. So there is a little bit of lag there. When one looks more closely at the curves for the higher temperatures, this lag can also be found there: the cooling down curves show a little bit narrower sub loops.

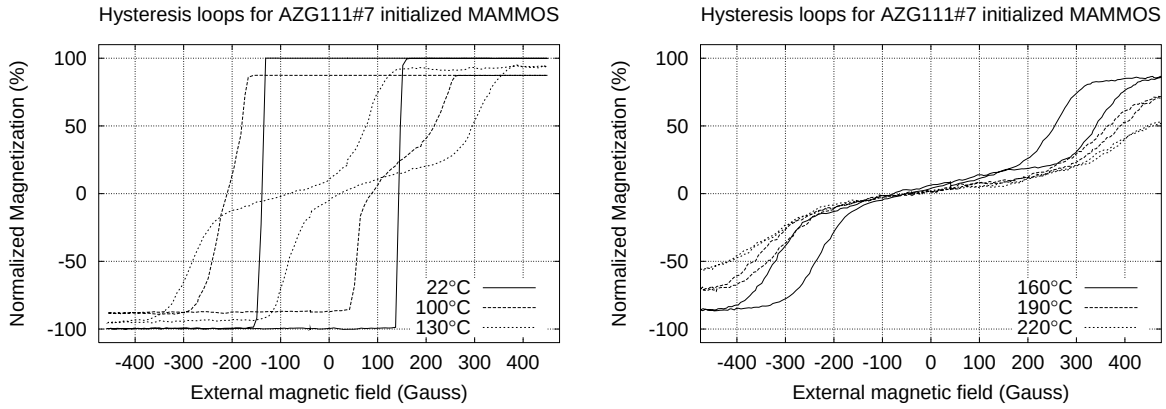

(a) (b)

Figure 3.9: Hysteresis loops of AZG111#7 for increasing temperature. The loops seem to split in two sub loops and the total magnetization decreases. Note the asymmetrical behavior.

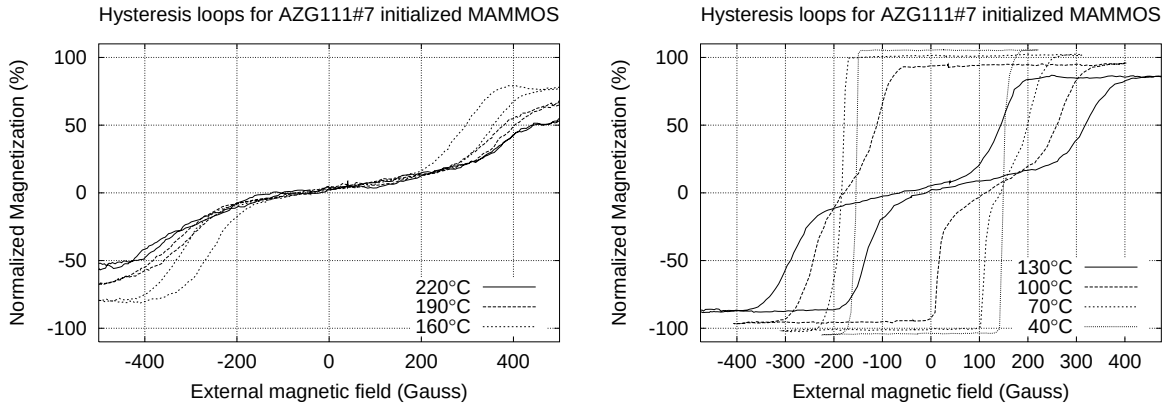

(a) (b)

Figure 3.10: Hysteresis loops of AZG111#7 for decreasing temperature. The behavior is almost identical to the behavior when heating up. Note again the asymmetry in the loops.

A general observation is that at a certain temperature the magnetization at remanence becomes zero, because of the splitting of the loops. This can be used to explain some effects discussed in section 3.3.4. The lag discussed above is also visible in this effect a little bit: when cooling down the magnetization at remanence is about 100 Gauss, while at heating up it is about 110 to 120 Gauss. Those differences might be linked to the differences in behavior discussed in the above mentioned section. The critical temperature for the appearance of domains in that section does not really conform with the temperatures found in these hysteresis loops. This can be caused by an aging effect of the sample. The measurement was done a couple of times before on the exact same sample and then this temperature was found to be a lot higher and very near the temperature found in the above mentioned section.

3.1.7 Summary/Conclusions

A MOKE set up was used to probe the magnetization of a MAMMOS read out layer in an externally applied magnetic field. Due to the used wavelength of 632 nm, only the transition metal (TM) component of the GdFeCo MO layer was probed. This resulted in hysteresis loops which appeared to be very rectangular at room temperature. The dependence on temperature of the hysteresis loops was measured with the help of a home made heating stage. This resulted in a behavior of the saturated magnetization M_s versus temperature (T) which was very much like the behavior of a ferromagnet. From those loops the coercive field H_c as a function of T could be extracted. The result was an almost linear decrease of H_c with increasing T. When cooling down, the loops show a slight deformation which could not clearly be explained. The M_s versus T curve also showed ferromagnetic behavior, but appeared to be different depending on how many times the sample was heated up. So a clear aging effect was observed. For a real MAMMOS application this aging is not so important, since the heating is then local and occurs in the nanosecond time regime.

The hysteresis loops measured a the real initialized MAMMOS sample showed a splitting of the loops when the temperature was increased. This seems to point to a double layer switching behavior (parallel, anti-parallel, parallel), but this could not be confirmed. The loops looked almost the same for cooling down, but again a deformation (asymmetry) of the loops was observed.

3.2 Time resolved measurements

As an investigation towards the main goal, the switching dynamics induced by 100 fs laser pulses of a MAMMOS readout layer has been investigated. At the same time, the breakdown of magnetization when reaching a temperature above Curie-point due to those laser pulses was observed.

The idea was to induce magnetization reversal by heating the sample locally while an external field is applied, which is lower than the coercivity of the sample. The heating with a laser beam will create a locally smaller coercivity and as a result the magnetization will reverse (i.e., thermo-magnetic writing, using a pulsed laser).

3.2.1 Set up

The sample that has been used is AZA161#7, as has been discussed in the previous section.

The set up used is again based on the polar Kerr effect. Time resolution was obtained by using a pump-probe technique. This means that the changes that are going to be measured are induced by a strong pump laser pulse. A much weaker probe laser beam that was split off from the main beam hits the sample after a variable delay (obtained by choosing a longer light path for this probe beam). The delay can be scanned by controlling the step motors of the delay line by a computer.

The set up is schematically depicted in figure 3.11. An amplified Ti-Sapphire

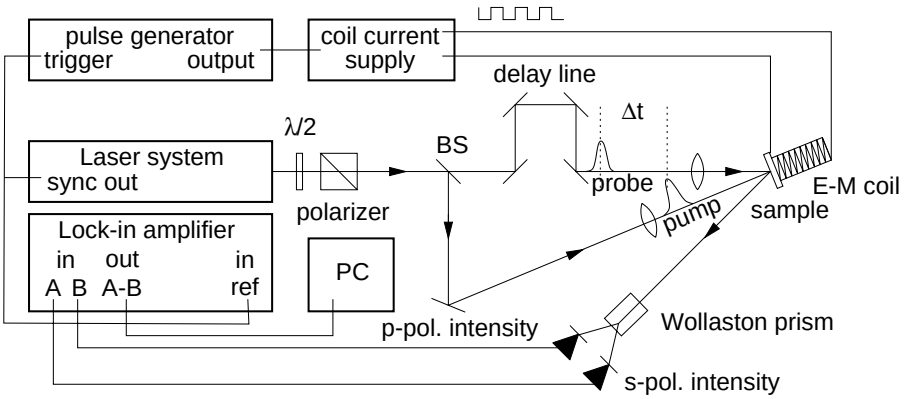

Figure 3.11: A scheme of the set up that was used for the time resolved measurements. See the text for an explanation.

laser system was used (Tsunami with the Spitfire amplifier, both by Spectra-Physics). It generates laser pulses of 100 fs duration at 800 nm wavelength. A repetition rate of 20 Hz was used. The energy per pulse could be varied with the help of an attenuation component (a Berek compensator was used in this case).

The pump beam was at normal incidence and focused to a spot of about 1 mm (FWHM), whereas the probe beam was incident on the sample at 30° and focused much tighter to approximately 70 μm. The probe pulses contained about 4×10^3 times less energy than the pump pulses. To achieve the best possible sensitivity and signal to noise ratio, a balanced diode scheme was used to detect the polar Kerr rotation only (not the ellipticity), as was introduced in [13]. Because of the used wavelength, only the TM component of the magnetization was probed.

The external field was applied along the easy axis perpendicular to the sample surface by mounting the sample on top of the soft iron core of a home made electromagnet.

To achieve a good signal-to-noise ratio it is necessary to average the signals of several probe-pulses without losing access to the dynamics of the effective field. This means the event that happens should be the same for every pump-probe

pulse pair. To create those same initial conditions before each pulse pair, an external field was applied at times between two subsequent pump-probe pulse pairs (from now on referred to as H_{off}) which was larger than the coercive field of the sample at room temperature ($H_{\mathrm{c}}(T_{\mathrm{room}})$), see also figure 3.12. In this way

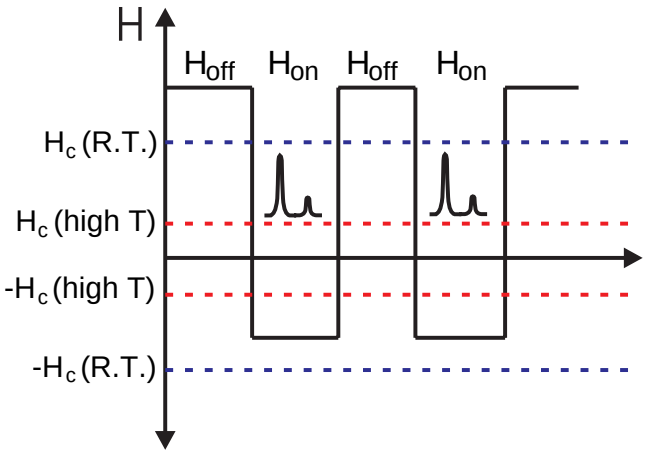

Figure 3.12: A schematic view on the oscillating external field configuration. This way the same initial conditions are created by erasing all magnetization before the arrival of the pump-probe pulse pair.

the magnetization of the sample was always saturated before each pump-pulse excitation, since the history of the magnetization is erased every time by an applied field that is larger than the coercivity at room temperature. So there is averaging without losing information about the coercivity (cf. figure 3.13). The magnetic field present when the pulse pair is interacting with the sample we call H_{on}. A slight disadvantage is that the continuous switching will probably make nucleation cores at points where local defects prevent the magnetization to be erased. However, in a real MAMMOS system, the same thing happens.

So, the resulting magnetic field was of a square-wave form. It was phase-locked to the laser repetition rate of 20 Hz by using the sync out of the laser system as a trigger for a pulse generator. This generator gives a square wave signal as output that was then fed to the input of the coil current supply (KEPCO BOP 36-5 bipolar operational power supply/amplifier), which transforms the square wave to current pulses: it has an voltage input (the 'control voltage') which is amplified to a current in the output. So when a square wave is put on the input, a square 'current wave' is generated at the output.

The low repetition rate was necessary to get real square field pulses. At higher frequencies the self inductance of the coil was too big to get this pulse shape. The square pulses ensure a constant magnetic field, alternating between two levels every cycle at 20 Hz.

Three configurations were chosen for H_{on} (which is again the direction and magnitude of the external field affecting the sample at times when pump- and probe-pulses were reflected at the sample):

1. $H_{\mathrm{on}} = H_{\mathrm{off}}$: the sample is always saturated

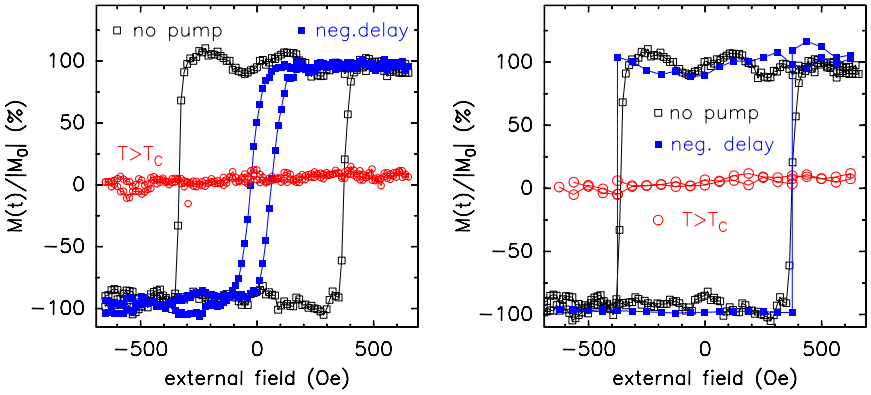

(a) (b)

Figure 3.13: Comparison of typical hysteresis loops measured by application of a quasi-static field (a) and by the application of the square wave field (b). For the first case, an apparent reduction of the coercive field is measured at negative pump-probe delay. This reduction reflects the fact that a reversed magnetization will be monitored by all subsequent probe pulses in case one preceding single pump-pulse initiated magnetization reversal.

2. $H_{\mathrm{on}} = -\frac{2}{3}H_c(T_{\mathrm{room}})$: there will be switching when the temperature is sufficiently increased

3. $H_{\mathrm{on}} = 0$: remanence

3.2.2 Results

For the three above mentioned configurations the results are discussed in this section.

3.2.2.1 Temperature induced magnetization dynamics

For the results mentioned in this section the first configuration was used. This means only the transient changes of the magnetization within a single domain state which are caused by transient electron- and lattice temperature are monitored. The external field suppressed any possibility of transient domain formation.

The results for a pump fluence of approximately $5.4\,\mathrm{mJ/cm^2}$ are shown in figure 3.14.

In the upper panel (a), the magnetization dynamics for both directions of the magnetization is shown next to the measured changes in linear reflectivity which monitor the time-evolution of the electron temperature T_e (see e.g [14] and references therein). A very fast and complete breakdown of magnetization during the first picosecond is observed, which is about 500 fs delayed with respect to the increase of T_e. The dynamics at a longer timescale is shown in the lower

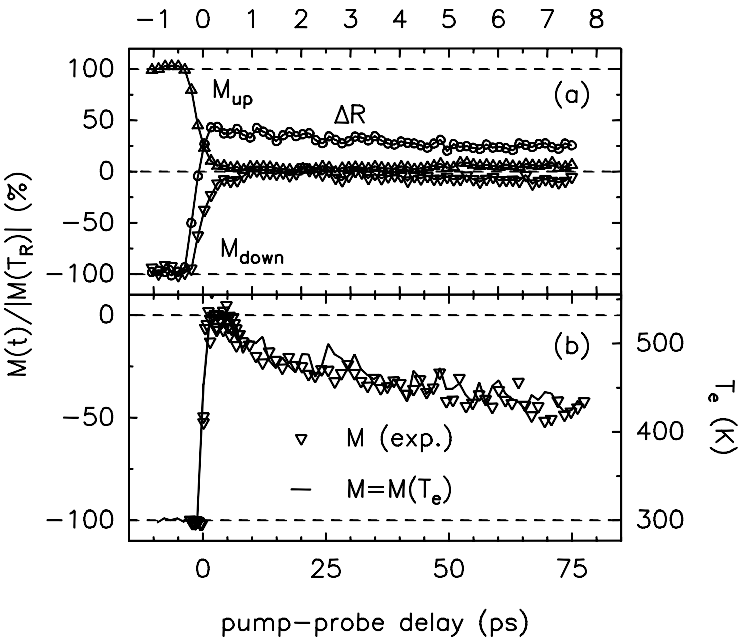

Figure 3.14: Magnetization of the TM susbsystem of GdFeCo normalized to its magnitude at room temperature as a function of pump-probe delay. Comparison of (a) the initial magnetization dynamics to simultaneously measured changes of linear reflectivity (ΔR) monitoring the transient electron temperature T_e, and of (b) the measured recovery of M at longer delays (symbols) to a theoretical expectation (solid line) which is obtained by transforming the measured $\Delta R(t) \propto T_\mathrm{e}(t)$ into $M(T_\mathrm{e}(t))$ via the equilibrium magnetization curve as is disussed in the text.

pannel (b) with the triangular symbols. The solid line in this graph shows the calculated behavior of the magnetization recovery. This calculation was done with the assumption that $M(t)$ is governed by the electron temperature via the equilibrium magnetization curve, which was measured in the previous section, see figure 3.7 (the earliest measured curve was taken, since that one was not yet affected by the heat treatment). The excellent agreement between the calculation and the measured data proves that the recovery of the magnetization is solely determined by cooling of electrons. This is in line with the behavior reported for ferromagnets in the literature (cf. [15–17] for example) and justifies the use of equation 2.17 to analyze transient magnetization reversal.

3.2.2.2 Fast magnetization reversal

To probe the dynamics of pump-pulse induced magnetization reversal, the second configuration is used: $H_\mathrm{on} = -\frac{2}{3}H_\mathrm{c}(T_\mathrm{room})$. The strength of the field was finetuned to prevent influence on the magnetization at negative pump-probe delay and still get a significant magnetization reversal within the investigated time range of 800 ps. To get both $M(t)$ (the magnetization, so the switching

behavior) and $M_0(t)$ (influence of temperature on the magnetization) the external field was periodically switched to the first configuration while scanning the pump-probe delay. This way we were sure the two curves were measured for the same environmental and initial conditions. Both are required for the interpretation with the help of equation 2.17.

The resulting data are compared to numerical solutions of equation 2.17 in figure 3.15. The figure shows it for five different pump fluences. The numerical

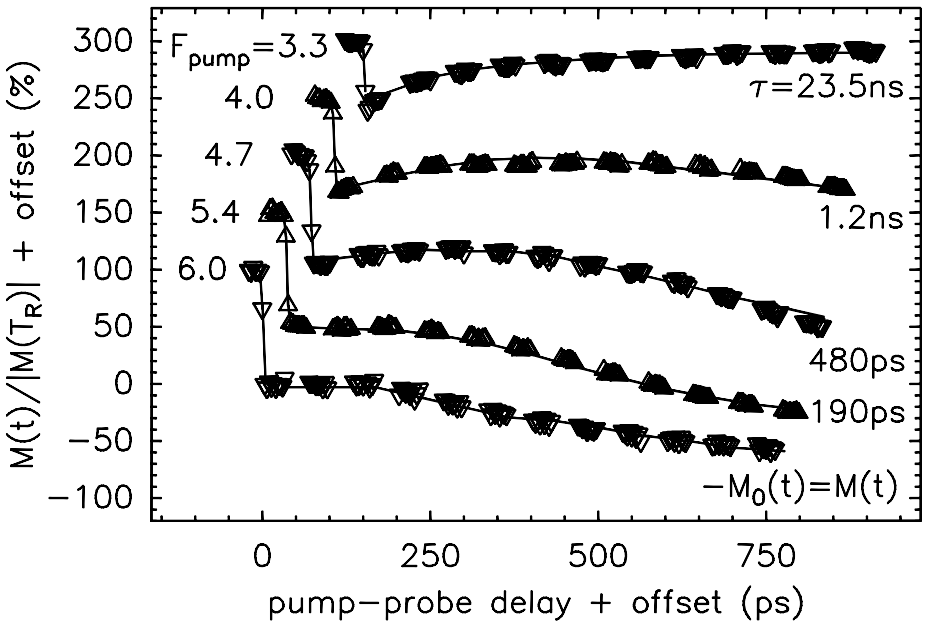

Figure 3.15: Transient magnetization reversal dynamics (symbols) measured for distinct pump fluences, F_{pump}. Solid lines represent best fits of equation 2.17 to the data. Values of F_{pump} (in units of mJ/cm^2) and the fitted reversal times τ are given. $M_0(t)$ was measured in the same runs, by periodically switching the phase of the current pulses, so that $H_{\mathrm{on}} = H_{\mathrm{off}}$, which yields in principle the same data as is shown in figure 3.14 and therefore it is not shown here. The data are offset along both axes for clarity.

solutions were obtained by taking $M_0(t)$ as the negative value of the actual magnetization measured for the external saturation field and treating only the 'reversal time' (which is actually the delay between the recovery- and reversal dynamics, see discussion in section 2.5) τ as a fit parameter.

As is clear, each individual data set is excellently fitted by the Bloch equation via one constant value of $\tau \pm 20\%$ despite the fact that the temperature varies over a large range up to 200 K. This finding proves that the temperature induced break down and recovery of the TM-magnetization as well as its reversal dynamics is comparable to the behavior of ferromagnets, since equation 2.17 does not take the coupling between the TM- and RE-moments into account.

The fitted 'reversal times' decrease strongly with increasing pump fluence (F_{pump}). A value of (190 ± 40) ps is found for $F_{\mathrm{pump}} = 5.4\,\mathrm{mJ/cm^2}$, where the

Curie-temperature is just reached within the probed area, but no delay between the recovery and reversal dynamics is found for a higher fluence of 6.0 mJ/cm^2, where also the surrounding of the probed spot is heated above T_C. These results show that the surrounding has a significant influence on the reversal dynamics and that the speed of thermo-magnetic writing is only limited by the cooling rate of the sample.

An additional point is the following. There is nothing known about the changes in the coercivity in the first few picoseconds. But since the reversal times are not a function of temperature, but only depend on the fluence, it is expected that the effective field (external field minus coercivity) will be constant in that time. This idea was checked by measuring hysteresis loops at distinct pump-probe delays. The results, which are presented in figure 3.16, indeed show that H_c remains zero for pump-probe delays up to 667 ps. Furthermore, the hysteresis

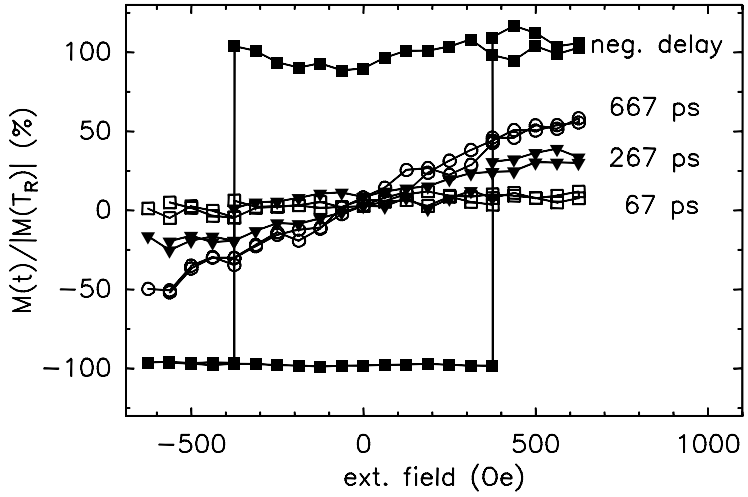

Figure 3.16: Hysteresis loops measured for a pump-fluence of 5.4 mJ/cm^2 at distinct pump-probe delays given in the figure. The loops demonstrate that the coercive field remains zero for pump-probe delays up to about 670 ps.

loops show a transition from rectangular shape at negative pump-probe delays (reversal within a single domain) to continuous changes of M with H at positive delays, which is characteristic for transient domain formation. Combining these observations with the behavior of τ, we suggest that the magnetization reversal is due to nucleation and growth of oppositely directed domains driven by the external field. The fact that the speed of the reversal process is increased when the pump-fluence is increased could be due to an increase in the number of initially created nucleation sites (breakdown due to oppositely oriented spins) and to a simultaneous decrease of the exchange coupling to the surrounding.

3.2.2.3 Dynamics of remanent magnetization

So far, pump-pulse induced magnetization dynamics which were controlled by an external field have been discussed. By comparing these results to data ob-

tained in remanence it can be elucidated whether the magnetization dynamics in remanence is determined by temperature effects only or whether it is also affected by transient domain formation. The data in figure 3.17, obtained for high pump-fluence, show that the dynamics in remanence is governed by a convolution of temperature and domain formation effects. This is supported by the perfect agreement of the dynamics observed in remanence and the solid line, representing the sum of the values obtained for $H_{\mathrm{on,sat}}$ and $H_{\mathrm{on,opp}}$.

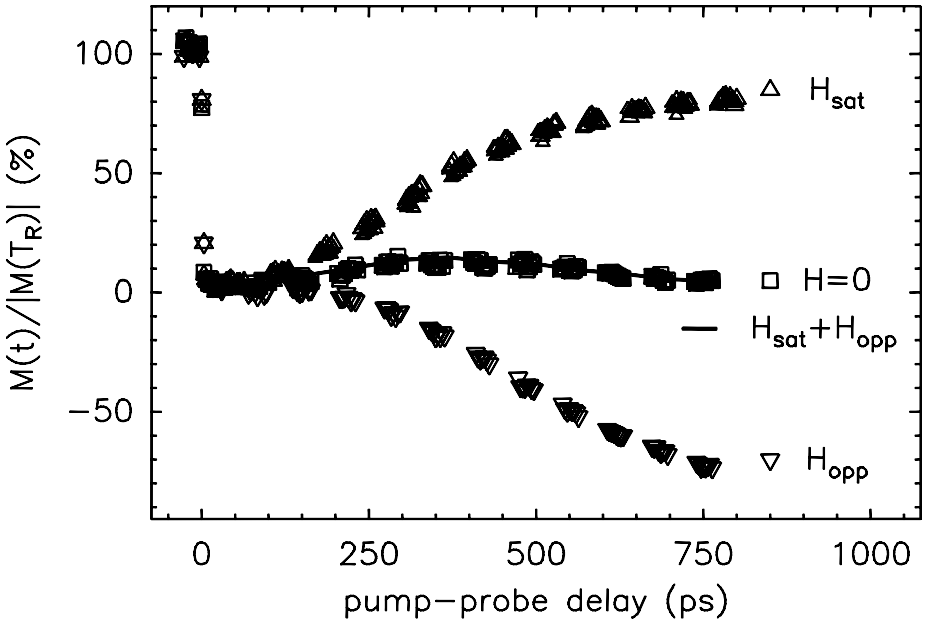

Figure 3.17: Comparison of magnetization dynamics measured for $F_{\mathrm{pump}} = 5.4\,\mathrm{mJ/cm^2}$ and: 1. $H_{\mathrm{on}} = H_{\mathrm{sat}}$, 2. $H_{\mathrm{on}} = H_{\mathrm{opp}}$ and 3. $H_{\mathrm{on}} = 0$. The solid line represents the sum of the values obtained for H_{sat} and H_{opp}.

3.2.3 Summary/Conclusions

It is believed that this is the first report of an observation of femtosecond pump-pulse induced magnetization reversal. For the TM-magnetization of ferrimagnetic α-$Gd_{23.1}Fe_{71.9}Co_{5.0}$ the reversal dynamics is perfectly described by an adapted version of the Bloch-equation. The corresponding reversal times do not depend on temperature, but decrease strongly with increasing excitation density. Even identical recovery and reversal dynamics were found for the highest pump-fluence. However, the observation of a finite reversal time of (190 ± 40) ps when the temperature within the probed area just exceeds T_{C} indicates significant influence of the colder surrounding. These results point to (sub)nanosecond bit access times in MAMMOS, since copying and amplification occur within about $1\,\mu$m spots at temperatures below T_{C}. The behavior of the reversal times as well as the shape of hysteresis loops measured at distinct pump-probe delays provide strong evidence that the magnetization reversal is due to transient domain

formation. Regarding the purely temperature induced magnetization dynamics, a fast and complete breakdown of M within the first picosecond is observed, which is about 500 fs delayed with respect to the equilibration of the electron gas. The recovery of M at delay times > 2 ps is uniquely related to T_e via the equilibrium magnetization curve. A comparison of temperature induced dynamics and of field-induced magnetization reversal to data obtained for the same high pump-fluence in remanence, demonstrates that the dynamics of remanent magnetization cannot be interpreted by temperature dynamics only.

3.3 Observation with polarization microscope

This section is mainly about the work done at Hitachi-Maxell Ltd in Japan. The goal was to investigate the domain structures of MAMMOS samples in detail with the help of MOKE microscopy. Several kinds of measurements have been done and are discussed below.

3.3.1 Set up

The set up is schematically depicted in figure 3.18. As is mentioned in the

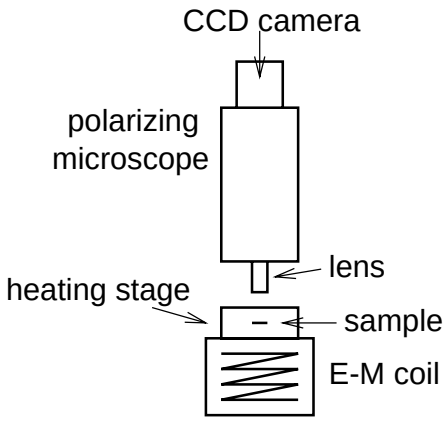

Figure 3.18: The setup that was used to make MO images. The sample was put inside a heating stage, which in turn was placed on an electromagnet. The axis of the magnet was perpendicular to the sample. The images are made with a polarizing microscope which had a CCD camera built in. A computer was used to optimize (most of the time only the contrast was enhanced) the images.

caption, it is possible to increase the temperature of the sample with a heating stage and apply a perpendicular external magnetic field with the electromagnet. Also, there is a small blue dye-laser available in the microscope to heat the sample locally, when required.

The external field is controlled by a current source. The current is controlled manually and can be read out on an analogue meter. There are some disadvantages of this:

- the current indicator is quite rough, its scale was from 0 to 10 A, so not very accurate for lower currents
- the actual field has to be extracted from the current via a calibration curve
- when increasing the field (thus current) until a certain event happens, the current will always be a little higher than the actual value at which the event happened due to human slowness (manual control) and the delay of the image (what is seen on the computer screen is always a little later than when it really happened, because of the integration time of the CCD camera and the processing time of the computer).

These disadvantages make the magnetic fields that are mentioned in the results somewhat inaccurate.

The images are a result of subtracting two images that were taken at the same angle with respect to the cross-polarized angle, but on different sides. This means the two pictures are inverted with respect to one another. Subtracting results in contrast enhancement and filters out any non-MO parts.

The resulting pictures were processed with the computer program used to retrieve them. Most of the time, only the contrast was adjusted. It was done in such way that the lightest (useful) parts were just not saturated and the same for the darkest parts. This gives the clearest images and uses all information available.

3.3.2 Samples

Several samples were investigated. The main samples were the AZG111-series. Those are MAMMOS samples. The layer structure can be found in figure 3.19.

The difference between the AZG111 samples #1 to #8 lies in the sputtering powers of the Gd and Tb. In table 3.1 is shown which samples have what sputtering powers. For these samples there were flat test pieces available which had

Table 3.1: AZG111-samples and their Gd(x)- and Tb(y) sputtering power.

Gd(↓)/Tb(→) power	$y =$ 1.2 kW	$y =$ 1.3 kW
$x = 1.0$ kW	#1	#5
$x = 1.1$ kW	#2	#6
$x = 1.2$ kW	#3	#7
$x = 1.3$ kW	#4	#8

a glass substrate and also a cd-sized disk was available on which real MAMMOS recording and readout could be tested.

Another sample that was used (initially to get started) was AXK291#2. This sample was a MAMMOS sample with a polycarbonate disk substrate. The readout layer had maze-shaped domains at room temperature and zero field.

There were more samples available, like AZA161#7, which was also used for the magnetization reversal dynamics measurements.

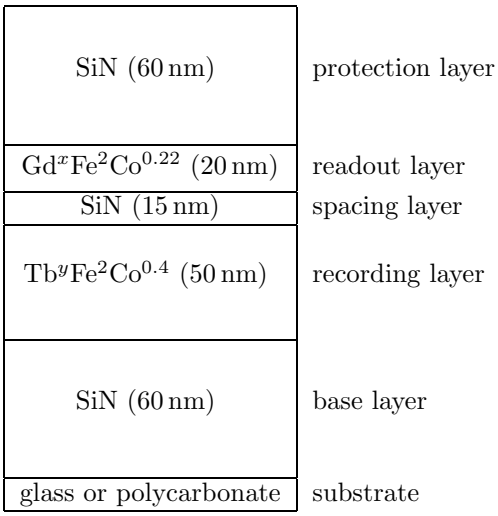

Figure 3.19: The structure of samples AZG111. Again, on the left the materials and thicknesses are indicated and on the right their function is mentioned. The sputtering powers for the components in the MO-alloys is given in kW; see the superscript numbers. The difference between the AZG111 samples is that the sputtering powers for Gd and Tb were varied (as is indicated by x and y, respectively), see table 3.1.

3.3.3 Difference land/groove and flat region switching

For these experiments, the AXK291#2 sample was used. The temperature was kept at R.T. In this experiment the variation of M with H_{ext} was investigated. A Kerr hysteresis loop of this sample showed that the switching of the magnetization occurred in two steps. Unfortunately, the graph of this loop is not available anymore, but it is sketched in figure 3.20. The goal was to find out with the microscope why this happened.

At first, the sample was put in a very strong say 'negative' magnetic field, to start with a certain magnetization. When the field was turned off, most of the initial magnetization-pattern returned, as this sample had a maze pattern at room temperature and zero field, see figure 3.21(a). Then, a 'positive' field was applied.

The results were quite clear: in the microscope's pictures could be seen that first, at around 20 Oe, the remaining remanence induced by the 'negative' field completely vanished, making the net magnetization (of the mazed part) zero. Then the main part of the sample switched quite early; not really square switching, but switching (of the mazed part) was complete near around 100 Oe (cf. figure 3.21(b)).

After getting saturation of the mazed part, the field was increased even further. Then, at a much higher field of 650 Oe, the rest of the sample started to switch (figure 3.21(c)). This switching occurred in the land/groove area (see section 1.1) of the sample. Complete saturation was achieved at 930 Oe.

In other words: the land/groove area of the sample has a much higher coer-

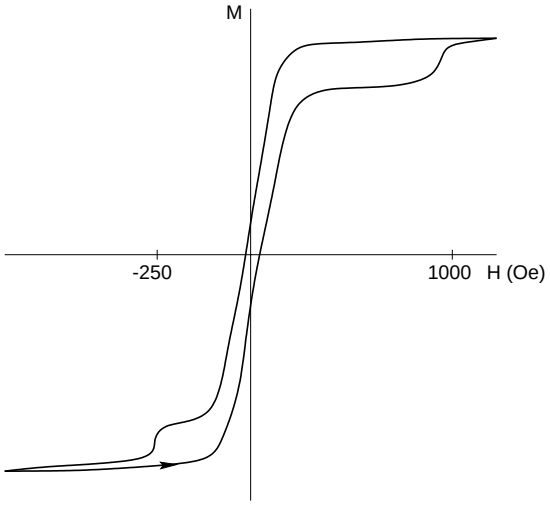

Figure 3.20: Sketch of the hysteresis loop of AXK291#2.

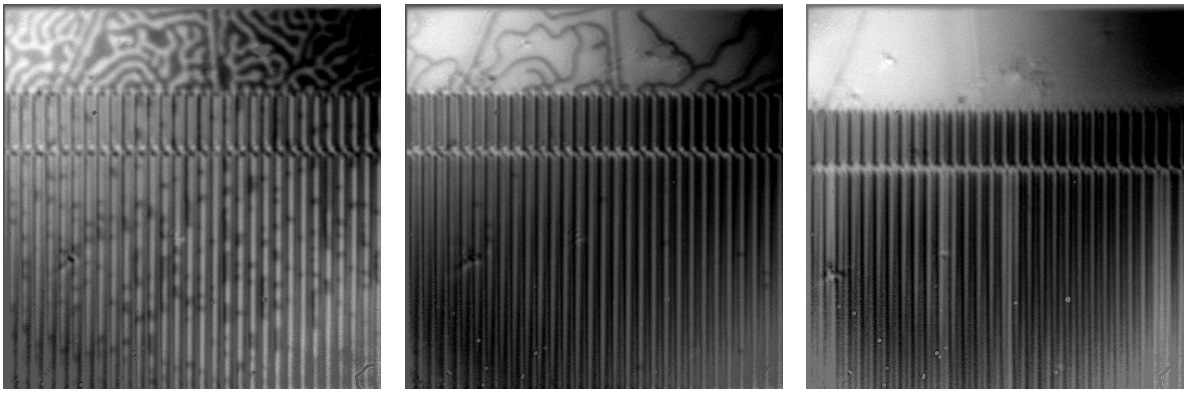

(a) $H_{\text{ext}} = 0\,\text{Oe}$ (b) $H_{\text{ext}} = 80\,\text{Oe}$ (c) $H_{\text{ext}} = 650\,\text{Oe}$

Figure 3.21: Difference in switching for flat and land/groove area in AXK291#2. At zero field the sample shows a mazed pattern of domains (a). 80 Gauss almost drives out all domains from the flat part (b) and at 650 Oe the land/groove part of the sample starts to switch (c). The image size is $50\times50\,\mu$m. Note that the strong color gradient on the flat part is due to inhomogeneous illumination.

civity than the other parts, since it switches a lot later. This can be explained if the structure of the land/groove part is looked at more closely. It is schematically depicted in figure 3.22. The sides of the land-parts are known to be a lot

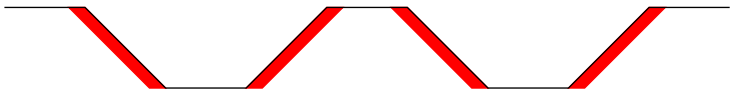

Figure 3.22: The land/groove structure of sample AXK291#2. The marked areas (the sides of the 'lands') are known to be quite rough, compared to the rest of the surface.

rougher than the rest of the surface. Because of the roughness there will be a lot more pinning, increasing indeed the coercivity, so it is probably those parts that switch so much later (i.e., have a much higher coercivity).

There is a problem however. If the sample is switched in the other direction, the same happens, but there the coercivity of the land/groove part is only 670 Oe; starting to switch at 300 Oe already. This asymmetry could not be explained.

An additional problem is that normally, pinning sites tend to 'catch' magnetization, i.e., once it has been magnetized, it is very hard to change it back. This normally helps a sample to change magnetization easier, since the site acts as a nucleation point.

3.3.4 "Thermal hysteresis" in initialized MAMMOS samples

In this subsection a special effect is discussed which was observed when an initialized MAMMOS sample like AZG111#3 or #7 was heated up and cooled down without applying an external field. All images of this section show a part of the sample that is about $70\times70\,\mu$m.

A MAMMOS sample which is not initialized (i.e., of which the recording layer is *not* in a single domain state), shows the following behavior when the temperature is increased (an example is shown in figure 3.23):

1. until a certain temperature nothing happens
2. above that temperature, 'grey' domains appear in the readout layer
3. those domains keep appearing (and appear faster when the temperature increases or when an external field is applied) until the whole picture is grey

This can be explained with the help of the hysteresis loops as a function of temperature (see section 3.1.5), if we assume they also apply for untreated, natural samples. At higher temperatures, the hysteresis loops have shifted upper and lower parts. The lower part is shifted to the left and the upper part to the right. At a certain temperature it is shifted so far that at zero external field the magnetization can go to zero, resulting in a grey area on the pictures (either in-plane magnetization or small maze pattern structures). In the meantime the stray field of the domains of the recording layer is increased, making nucleation easier. There can be quite high stray fields locally, since the sample's recording

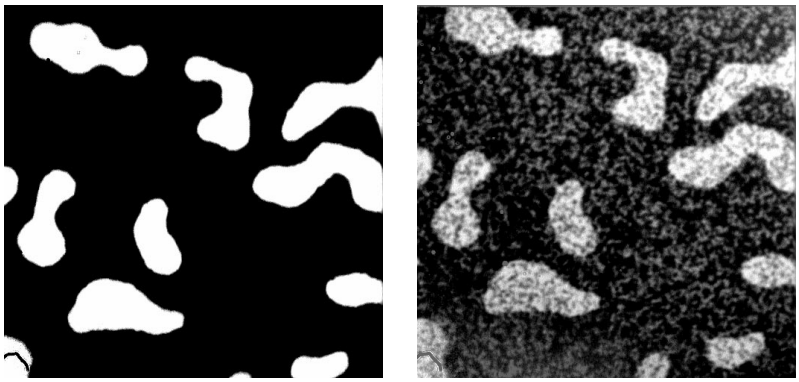

(a) $T < 196°\mathrm{C}$ (b) $T = 196°\mathrm{C}$

Figure 3.23: AZG111#4, (a) before reaching the 'critical temperature' for formation of grey-looking domains and (b) at this temperature. The domains visible in (a) and partly in (b) are natural domains, i.e., they were there before doing anything to the sample after it was sputtered.

layer is not initialized and may thus have a wild pattern of domains (it has been observed that the read out layer of a fresh sample had such a pattern).

If then a field is applied, the material moves even closer to the splitted part of the loop, where the magnetization is close to zero. So it will indeed increase the effect.

An example of this behavior is shown in figure 3.23. There the 'critical temperature' for the appearance of domains was 196°C for the used sample AZG111#4.

At some point the whole sample is covered with the grey domains. When it is cooled down, the grey domains gradually turn into black and white domains, showing an extremely distorted version of the initial magnetization state of the readout layer. An example of this is shown in figure 3.24.

For samples AZG111#3 and #7 an additional feature was added: while the sample was at a high temperature (well above this 'critical temperature') an external magnetic field was applied to initialize the recording layer. After this, the external field was turned off during the rest of the experiments (except to initialize the readout layer, see below). The acquired initialized sample was then cooled down.

The following experiment was then done with such a sample:

1. initialize the sample's readout layer (in the opposite direction of the initialized recording layer) and turn off field; all at room temperature
2. increase temperature until about 230°C
3. decrease temperature back to room temperature

This experiment yielded quite interesting results. What happens is described in table 3.2 and the corresponding images can be found in figure 3.25.

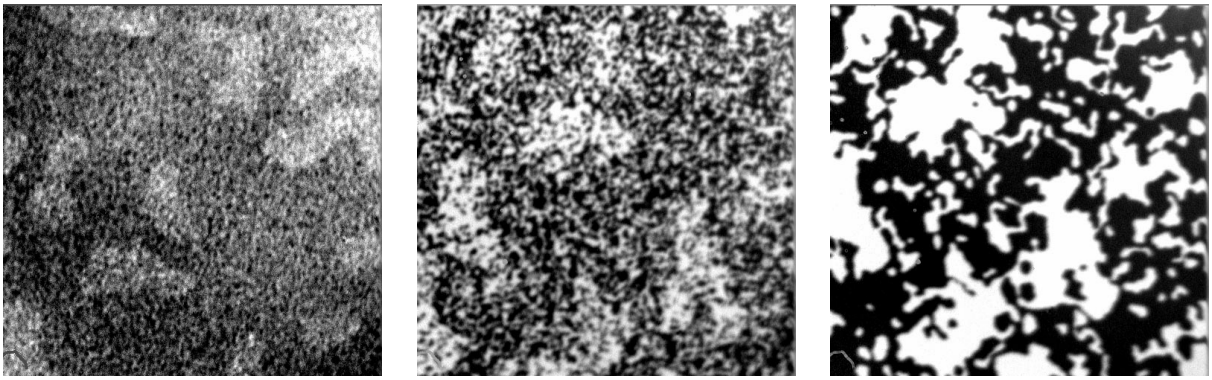

(a) $T = 196°\mathrm{C}$ (long t) (b) $T = 68°\mathrm{C}$ (c) $T = 26°\mathrm{C}$

Figure 3.24: AZG111#4, (a) after staying a while at 196°C (b) return of black and white domains (c) returned at roomtemperature where a distorted version of the initial pattern is left (cf. figure 3.23 of which this figure is a continuation).

Table 3.2: Description of what happened during the experiment described in the text for sample AZG111#7. The images can be found in figure 3.25.

T (°C)	observations/comment
Heating up	
26-145	Nothing happens. Readout layer remains fully white
146	Appearance of round domains of 1.5 μm diameter
160-170	More and more domains appear
175	Shape changes a little: elongation and 'tentacle' formation
180	'Tentacles' become paths (1 μm wide), connecting initial domains
182-230	'Maze' formed by paths becomes denser and denser
198	Paths seem to get thinner, as density is still increasing
205	Density increasing, width of white leftover parts decreasing
210-215	As this continues, the structure gets below resolution
220-230	All structure below resolution. Looks greyish.
Cooling down	
230-205	Nothing visible until 205°, where structure is getting resolved again
200	Visibility of high-density maze pattern becomes better and better
190	Pattern resolved again; preferred direction for domains visible!
180	Black/white equal again; preferred direction very clear from here
170-70	White part grows continuously; stripes reduce to dots as dots vanish
110	Only some dots left, all stripes have been reduced to dots
110-70	Dots disappear slowly to vanish completely at 68°C

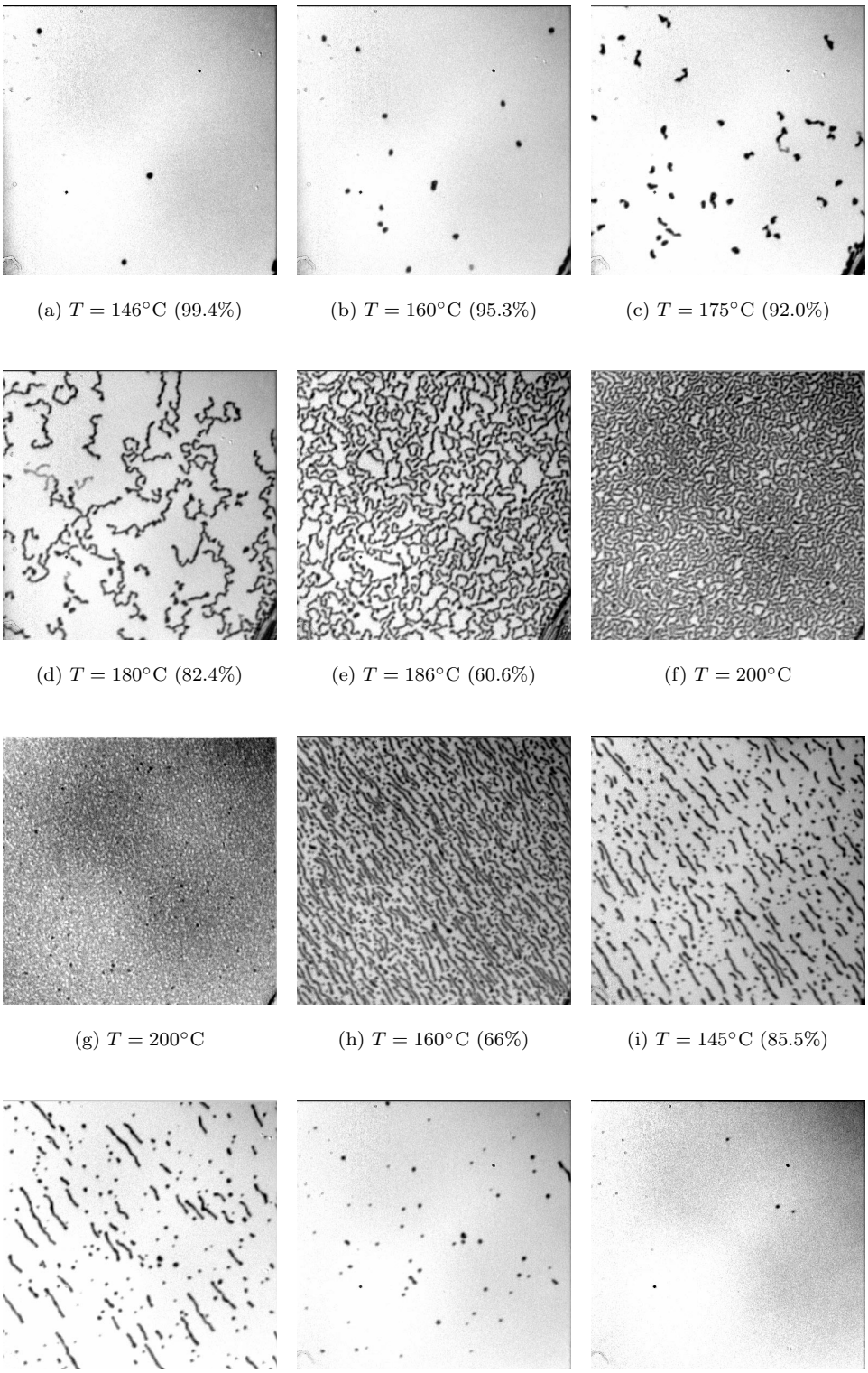

(a) $T = 146°C$ (99.4%) (b) $T = 160°C$ (95.3%) (c) $T = 175°C$ (92.0%)

(d) $T = 180°C$ (82.4%) (e) $T = 186°C$ (60.6%) (f) $T = 200°C$

(g) $T = 200°C$ (h) $T = 160°C$ (66%) (i) $T = 145°C$ (85.5%)

(j) $T = 130°C$ (94.8%) (k) $T = 110°C$ (99.1%) (l) $T = 70°C$ (99.5%)

Figure 3.25: Thermal hysteresis in AZG111#7: heating up (a)-(f) and cooling down (g)-(l) shows asymmetry. Between (f) and (g) the temperature has been up to 230°C. When it was possible to extract it, the percentage 'white' is between parentheses.

The main points are, for heating up:

1. at a certain temperature, there is nucleation of opposite domains
2. those domains grow in a random-walk way, making 'paths'
3. stripes get so dense that they drop below resolution.

And for cooling down:

1. when the fine pattern gets resolved again, it seems to consist of stripes that are aligned in a certain direction
2. as the temperature goes down, more and more stripes disappear; domains get smaller
3. at a certain temperatures, all domains are gone.

It is clear that there is an asymmetry between heating up and cooling down. For that reason this effect was called 'thermal hysteresis in initialized MAMMOS media'.

The other sample (AZG111#3) that was given the same treatment showed very similar behavior. Some differences were that the temperatures at which things happen were a little different, also due to the fact that there was a big scratch in the observed region:

- heating up:
  - 153-175°C: scratch shows opposite domains (formation and growth)
  - 180°C: stripes growing from scratch
  - 215°C: fine structure drops below resolution
- and cooling down:
  - 190°C: preferred direction of domains visible
  - 60°C: all free domains disappeared
  - 26°C: still some domains around scratch

Another clear difference is the shape of the domains when cooling down. They are not so regular as in AZG111#7. This can be seen in figure 3.26.

The general observation can be explained as follows. As usual, the coercivity of the readout layer is decreasing with increasing temperature and the magnetization of the recording layer is increasing. So at a certain temperature, there will be nucleation of oppositely magnetized domains in the readout layer, at positions where the local coercivity is even lower than the already lower coercivity of the surroundings. This is mainly caused by the huge demagnetizing energy and the small K_u, the latter making the domain wall energy low, enabling the formation of domain walls. Then, there is more nucleation and growth of the existing domains, connecting existing nucleation points. It is clear that the sample seems to prefer dendritic stripe growth above a large domain configuration with wall motion. Apparently the demagnetization energy is too high for this and thus, the domain is splitted in the dendritic stripes to minimize this energy. (Similar behavior for certain Co/Pd multilayers was reported in [18] and in [19]

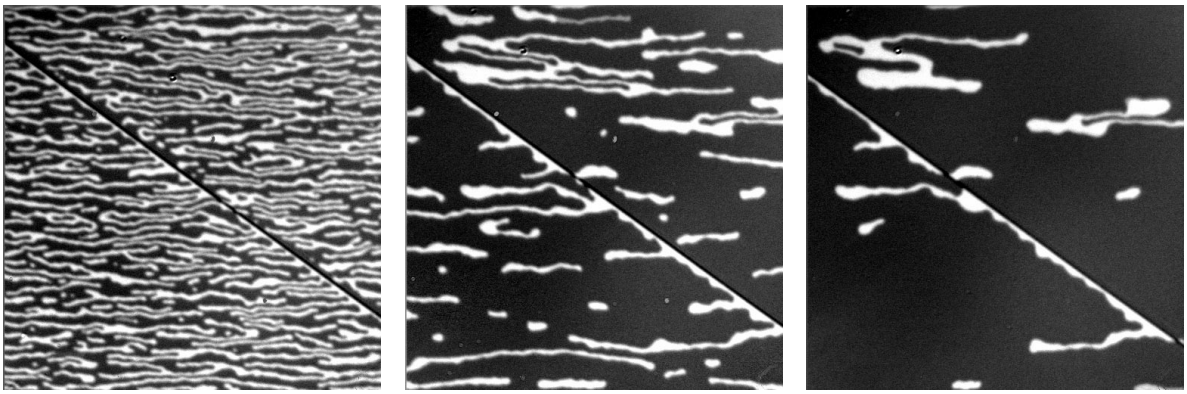

(a) $T = 155°C$ (38% white) (b) $T = 120°C$ (19%) (c) $T = 100°C$ (8.5%)

Figure 3.26: Some pictures of the cooling phase of AZG111#3, to compare with the pictures of figure 3.25. The shape of the domains is quite different here.

also the difference between nucleation- and wall-dominated reversal is shown for Au/Co/Au samples with different thicknesses.) Because of the higher energy at the ends of a non-circular shaped domain (the more curvature, the higher the energy), the stripes tend to expand at those points. The only problem is that the recording layer was initialized in the direction which shows black on the pictures. So, how those white domains appear is unclear. It can not be just copying. Maybe just the high demagnetizing energy is responsible for it.

This network of dendritic stripe domains is extended until the structure is so fine that it drops below resolution. When the temperature is reduced again, it is clear that the domains are aligned in a certain direction. This is most likely caused by an in-plane external field, originating from remanence in the pole piece of the electromagnet. This behavior could be confirmed by applying an external in-plane field with a permanent magnet to a (different) sample: the domains now became aligned with the field lines of that magnet. This indicates that the domain walls are very mobile at the higher temperatures (probably alignment only happens at the highest temperatures reached in the experiment); there is no pinning anymore. At those temperatures the in-plane component of the domain-walls (in the middle of them) is apparently large enough to align itself with the weak external field. To achieve this, it is of course needed that the direction of the spins inside the domain wall change direction at two points. This involves having a pair of Bloch lines in the domain wall. See figure 3.27 for an illustration of this.

The last thing to explain is why the state of the readout layer returns to the initial, single domain state. It is clear that the domains become unstable at lower temperatures so that they collapse. The reason for that could be the following: as the temperature goes down, K_u increases again, making the domain wall energy higher. This makes the single domain state more favorable than the multiple domain state: the domain walls shrink and make the domains collapse to get in a lower energy state.

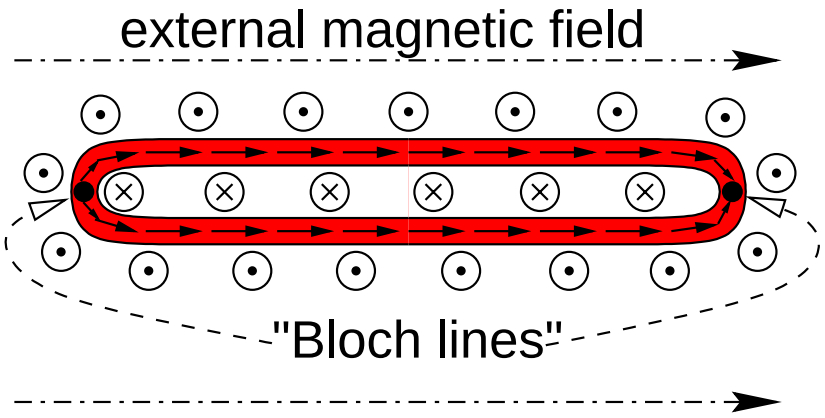

Figure 3.27: A schematic view of a single magnetic domain having perpendicular magnetization. The magnetization of the domain is pointing into the paper while the magnetization outside the domain is pointing out of the paper. The colored/darkened region between the domain and the outer area is the Bloch-type domain wall, which has an exagerated width here, for clarity. The spin direction in the middle of the wall is in-plane. The external magnetic field could have caused alignment of the domain by the magnetic moment exerted on the in-plane component of the domain wall at high temperature. For this to happen, it is necessary that the spin direction inside the wall changes orientation 180° at least twice. This is possible with a pair of Bloch lines, since at a Bloch line this is the case. For a thorough discussion of Bloch lines, see [20], chapter 4.

3.3.5 Copying and collapse of recorded domains

The last series of experiments with the microscope was done on the samples AZG111#2 and AZG111#3. The samples had recorded domains (of several sizes) in their recording layers. The goal was to look at the properties of domain collapse and copying in those samples. The coupling strength between recorded and copied domains could be investigated as a function of temperature. Also, the influence of the stray field and the coercivity as a function of temperature could be looked at. This was all done by applying an external field to the samples and looking what happens to the magnetization pattern for different temperatures and fields.

The recorded pattern is schematically drawn in figure 3.28. The pattern

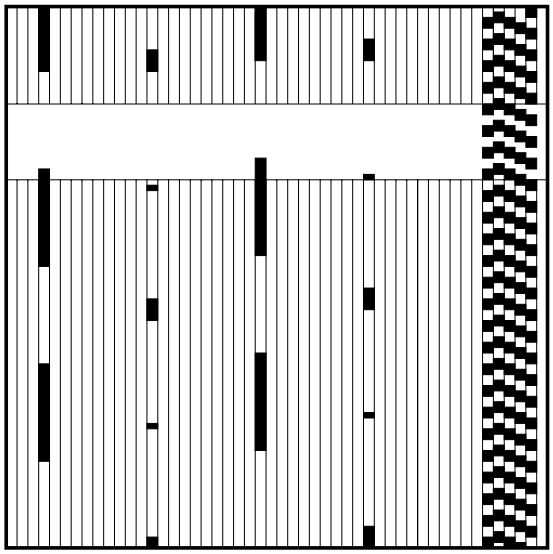

Figure 3.28: Schematical representation of the pattern that was recorded in the recording layer. The colours correspond to the ones on the pictures; so the initialization was done in the direction corresponding to white and therefore the recorded domains are black.

was chosen like this to have a good spacing between the different domains and also to have various sizes. The smallest domains were about 0.6 μm long. The pattern on the right was a test pattern to be able to find the recorded area back. The dimensions of the pictures are again 70×70 μm.

The procedure was as follows:

1. initialize readout layer in black direction
2. increase H_{ext} until a certain event takes place (then the field is noted and pictures are sometimes made)
3. after saturation (the picture shows completely white), decrease the field and do the same

The events that were noted are shown in figure 3.29. Of course the resulting fields are not very accurate, as is explained before. The last picture in that figure shows an interesting feature: the first part of the domain that returns is the outer part, at the domain boundary, showing as the black contours. This indicates that at this temperature the stray field is so strong (especially at the domain boundaries, since there a closed flux loop can be made) that it induces domain reversal in the read out layer, restoring the original domain there.

The results for AZG111#2 have been put in a graph, which is shown in figure 3.30. The following things can be seen in that graph:

- 'start reversal' and 'only copied domain pattern left' decrease with temperature. This means the coercivity is decreasing, as is expected
- 'start recovery' is increasing with temperature, representing the stronger magnetization and thus stray field of the recording layer. Also this behavior is expected. The values indicate what field is at least necessary to counteract this stray field, so it will be close to the stray field itself
- the 'collapse' curves show all (roughly) the same trend, but have a different offset. An exception is that the bigger domains seem to be more stable at temperatures above 100°C

For AZG111#3 the same kind of experiment was done. The results can be seen in figure 3.31. This shows basically the same behavior as AZG111#2, except that the temperatures at which the events occur are all shifted about 20 to 30°C (roughly, it seems to vary a little) and the maximum fields are higher (to get complete collapse). The latter may be due to local higher coercivities.

3.3.6 Summary/Conclusions

Domain structures in MAMMOS samples have been investigated with MOKE microscopy using static magnetic fields and temperatures. A difference in switching behavior for land/groove and flat parts of a MAMMOS sample was observed. The switching in the land/groove part was delayed a lot with respect to switching in the flat area. This was probably caused by pinning in that region due to higher roughness. An asymmetry between positive and negative field could not be explained. For initialized MAMMOS samples a 'thermal hysteresis' effect was observed. When heating up a sample in single domain state at a certain temperature, opposite domains nucleate and grow to a dense dendritic maze pattern as the temperature rises. When cooling down an aligned pattern of stripe domains was observed which disappeared gradually as the temperature decreased. The alignment is probably due to a small in-plane magnetic field of the pole-piece of the used magnet, acting on the in-plane component of magnetization in the domain walls. Copy- and collapse phenomena in MAMMOS disks have also been looked at. Domains of various sizes were recorded on the disk and the behavior of the read out layer was studied as a function of temperature and external magnetic field. The results were as expected: copying occurred at higher temperatures and/or at higher fields and a strong coupling between the read out layer and the recording layer was observed at higher temperatures due to the big stray field. This could also be seen in the contours of magnetic domains that were left over when the domain collapsed: the domain boundaries have the highest stray field.

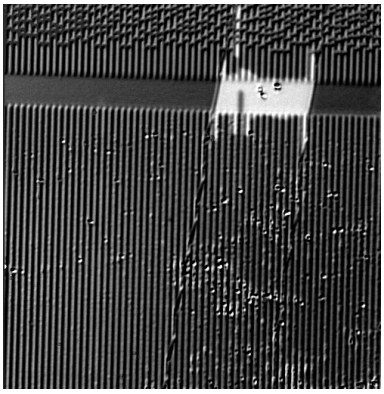

28°C, 30 Oe
start of reversal
(flat or L/G part)

(no picture; e.g., 28°C, 70 Oe)
recorded pattern visible

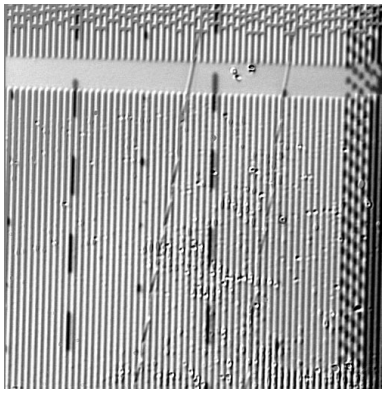

28°C, 125 Oe
only recorded pattern left

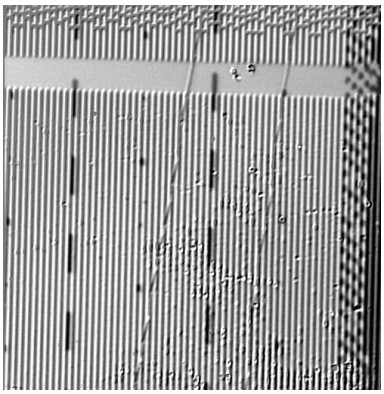

28°C, 135 Oe
test pattern domains collapse

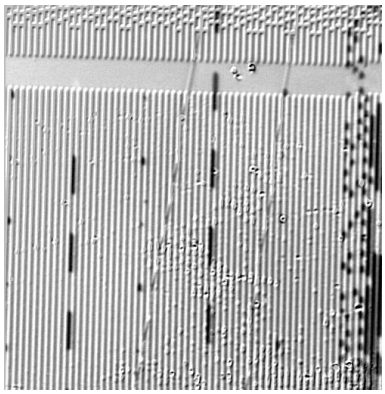

28°C, 150 Oe
long domains collapse

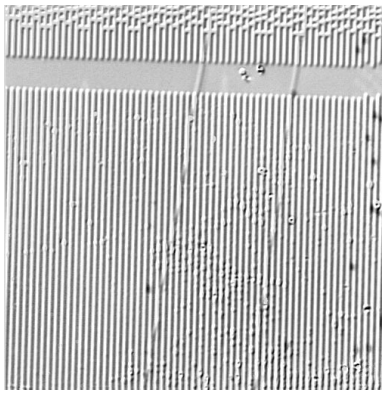

28°C, 170 Oe
almost all collapsed

(no picture; e.g., 28°C, 190 Oe)
all collapsed

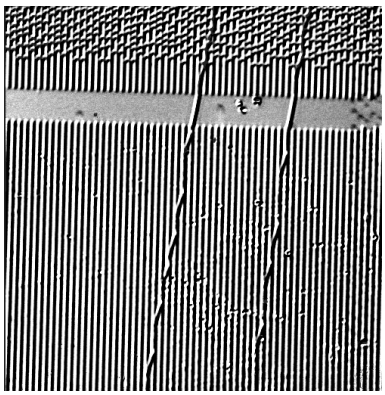

120°C, 200 Oe
recovery when decreasing H_{ext}

Figure 3.29: Examples of some events that occur when the applied field is changed. The last picture shows what happens if the field is decreased (after having every black domain collapsed first) at higher temperatures. Note that in this image, it can be seen that the first part of the domains that return is the domain edge. This shows as the black contours in the picture (look at the flat part). This is due to the strong stray field at domain boundaries.

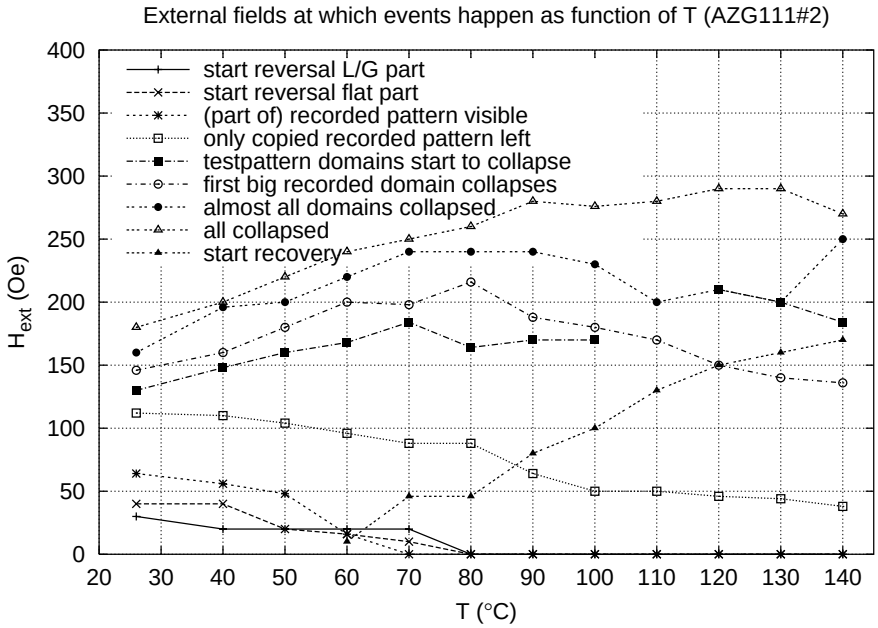

Figure 3.30: Noted events as a function of temperature for AZG111#2.

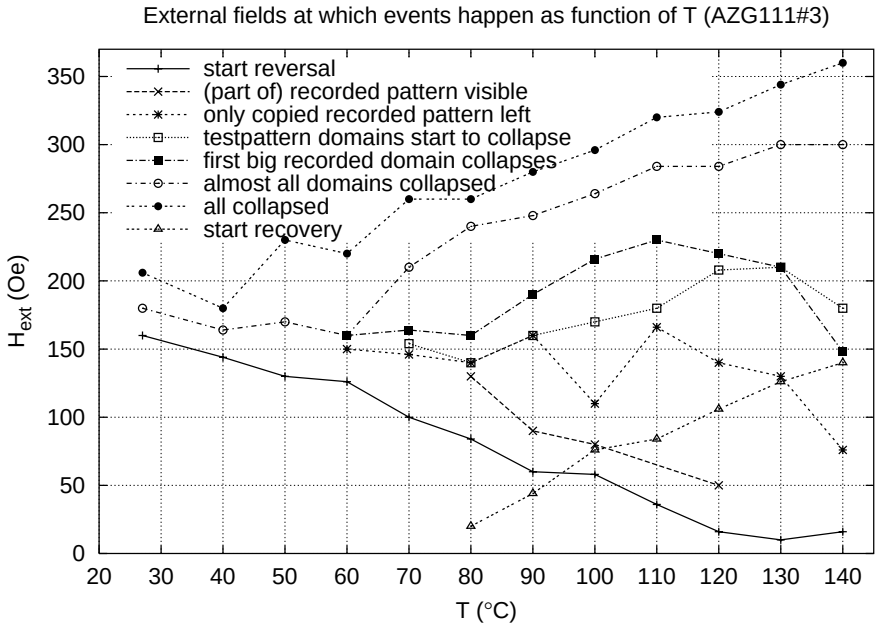

Figure 3.31: Noted events as a function of temperature for AZG111#3.

Chapter 4

Summary, conclusions and outlook

4.1 Summary and conclusions

The goal of the research reported in this thesis was to investigate some physical properties of MAMMOS: the Magnetically AMplified Magneto Optical System. A normal MO read out system uses one MO layer, limiting the bit size to the laser spot size (diffraction limit). But MAMMOS uses an extra read out layer in which tiny recorded bits that are much smaller than the diffraction limit are copied and expanded to the laser spot size with the help of an external field.

The research consisted of three parts: statical measurements (hysteresis loops) of the MAMMOS read out layer and a complete MAMMOS sample, time resolved measurements of the magnetization (reversal) dynamics and magneto-optical microscopy.

For the first part a MOKE set up was used to probe the magnetization of a MAMMOS read out layer in an externally applied magnetic field. Due to the used wavelength of 632 nm, only the transition metal (TM) component of the GdFeCo MO layer was probed. This resulted in hysteresis loops which appeared to be very rectangular at room temperature. The dependence on temperature of the hysteresis loops was measured with the help of a home made heating stage. This resulted in a behavior of the saturated magnetization M_s versus temperature (T) which was very much like the behavior of a ferromagnet. From those loops the coercive field H_c as a function of T could be extracted. The result was an almost linear decrease of H_c with increasing T. When cooling down, the loops show a slight deformation which could not clearly be explained. The M_s versus T curve appeared to be different depending on how many times the sample was heated up. So a clear aging effect was observed. For a real MAMMOS application this aging is not so important, since the heating is then local and occurs in the nanosecond time regime.

The hysteresis loops measured for the real initialized MAMMOS sample showed a splitting of the loops when the temperature was increased. This seems to point to a double layer switching behavior (parallel, anti-parallel, parallel), but this could not be confirmed. The loops looked almost the same for cooling down, but again a deformation (asymmetry) of the loops was observed.

In the second part of the research, magnetization reversal induced by a femtosecond pump-pulse is investigated on a GdFeCo MAMMOS read out layer, using the polar MOKE in a pump-probe set up. For the TM-magnetization of this ferrimagnetic material the reversal dynamics is perfectly described by an adapted version of the Bloch-equation. The corresponding reversal times do not depend on temperature, but decrease strongly with increasing excitation density. Even identical recovery and reversal dynamics were found for the highest pump-fluence. However, the observation of a finite reversal time of (190 ± 40) ps when the temperature within the probed area just exceeds T_C indicates significant influence of the colder surrounding. These results point to nanosecond bit access times in MAMMOS, since copying and amplification occur within about $1\,\mu$m spots at temperatures below T_C. The behavior of the reversal times as well as the shape of hysteresis loops measured at distinct pump-probe delays provide strong evidence that the magnetization reversal is due to transient domain formation. Regarding the purely temperature induced magnetization dynamics, a fast and complete breakdown of M within the first picosecond is observed, which is about 500 fs delayed with respect to the equilibration of the electron gas. The recovery of M at delay times > 2 ps is uniquely related to T_e via the equilibrium magnetization curve. A comparison of temperature induced dynamics and of field-induced magnetization reversal to data obtained for the same high pump-fluence in remanence, demonstrates that the dynamics of remanent magnetization cannot be interpreted by temperature dynamics only.

The third part consisted of an investigation of domain structures with MOKE microscopy using static magnetic fields and temperatures. A difference was observed in switching behavior for land/groove and flat parts of a MAMMOS sample. The switching in the land/groove part was delayed a lot with respect to switching in the flat area. This was probably caused by pinning in that region due to higher roughness. An asymmetry between positive and negative field could not be explained. For initialized MAMMOS samples a 'thermal hysteresis' effect was observed. When heating up a sample in single domain state at a certain temperature, opposite domains nucleate and grow to a dense dendritic maze pattern as the temperature rises. When cooling down an aligned pattern of stripe domains was observed which disappeared gradually as the temperature decreased. The alignment is probably due to a small in-plane magnetic field of the pole-piece of the used magnet, acting on the in-plane component of magnetization in the domain walls. Copy- and collapse phenomena in MAMMOS disks have also been looked at. Domains of various sizes were recorded on the disk and the behavior of the read out layer was studied as a function of temperature and external magnetic field. The results were as expected: copying occurred at higher temperatures and/or at higher fields and a strong coupling between the read out layer and the recording layer was observed at higher temperatures due to the big stray field. This could also be seen in the contours of magnetic domains that were left over when the domain collapsed: the domain boundaries have the highest stray field.

4.2 Further research

In this thesis two main methods are presented: MOKE for hysteresis loops and time resolved studies of magnetization and MOKE for domain observations with

microscopy. A next step would be to combine them in time resolved MOKE microscopy to study real time MAMMOS copy- and expand phenomena. This would then lead to an observation of the domain expansion speed, which was the original goal of the project.

Apart from that, also the individual parts can be expanded. There are already solid plans to look at more samples with the time resolved measurements. Examples are samples of the recording layer, samples with a thick gold substrate (i.e., a huge heat sink to see what happens to the switching behavior when the cooling is much faster) and samples with a different composition of the GdFeCo.

Also in the static microscopy measurements there could be done a lot more interesting experiments: a more thorough investigation of the discussed thermal hysteresis, especially for more different kinds of samples. It would also be good to do microscopy on the recording layer, to see what happens with it during this thermal hysteresis. General investigations on the effect of annealing could be made too. Aging effects caused by elevated temperatures were obviously not negligible. Further more, the dependence of the domain size in the copy- and collapse experiment could be investigated more thoroughly. In this context an investigation of the dependence of the domain shape could also prove interesting, since the stray field is highly influenced by this.

To expand the research with the CW MOKE, it would be interesting to use a light source that can probe the RE component of the ferrimagnetic material and see what happens there. This could also be done for the time resolved measurements of course.

It is clear that a lot of research is needed to get a good idea of what really happens in MAMMOS. Also to make it really work (and optimize the conditions) will take a great effort. From a fundamental point of view a lot can be learned about the used materials and layer structures and the complicated physics that is involved.

Bibliography

[1] M. Mansuripur, *The Physical Principles of Magneto-optical Recording*, Cambridge University Press, 1995.

[2] H. Awano, S. Ohnuki, H. Shirai, and N. Ohta, Appl. Phys. Lett. **69**, 4257 (1996).

[3] J. P. Jakubovics, *Magnetism and Magnetic Materials*, Cambridge University Press, second edition, 1994.

[4] C. Kittel, *Introduction to Solid State Physics*, John Wiley & Sons, third edition, 1966.

[5] S. Chikazumi, *Physics of Magnetism*, John Wiley & Sons, 1964.

[6] T. Katayama, M. Miyazaki, H. Arimune, and T. Shibata, J. Magn. Soc. Jpn. **8**, 121 (1984).

[7] P. Hansen, J. Appl. Phys. **62**, 216 (1987).

[8] M. Mansuripur and G. A. N. Connell, J. Appl. Phys. **55**, 3049 (1984).

[9] N. Rizzo, T. Silva, and A. Kos, Phys. Rev. Lett. **83**, 4876 (1999).

[10] R. Leermakers, A magneto-optical study of Co on step bunched vicinal stubstrates, Master's thesis, University of Nijmegen, Solid State Physics 2, 2000.

[11] A. Zvezdin and V. Kotov, *Modern Magnetooptics and Magnetooptical Materials*, Studies in Condensed Matter Physics, Institute of Physics Publishing, Dirac House, Temple Back, Bristol BS1 6BE, UK, 1997.

[12] K. Bennemann, *Nonlinear Optics in Metals*, International series of Monographs on Physics, Oxford University Press, 1998.

[13] M. Freeman, R. Ruf, and R. Gamabino, IEEE Trans. Magn. **27**, 4840 (1991).

[14] J. Hohlfeld, *Ultrafast Electron-, Lattice- and Spin-Dynamics in Metals*, PhD dissertation, Freie Universität Berlin, Berlin, 1998.

[15] A. Scholl, L. Baumgarten, R. Jacquemin, and W. Eberhardt, Phys. Rev. Lett. **79**, 5136 (1997).

[16] E. Beaurepaire, J.-C. Merle, A. Daunois, and J.-Y. Bigot, Phys. Rev. Lett. **76**, 4250 (1996).

[17] J. Hohlfeld, E. Matthias, R. Knorren, and K.-H. Bennemann, Phys. Rev. Lett. **78**, 4861 (1997).

[18] S.-B. Choe and S.-C. Shin, Phys. Rev. B **57**, 1085 (1998).

[19] J. Pommier, P. Meyer, G. Pénissard, and J. Ferré, Phys. Rev. Lett. **65**, 2054 (1990).

[20] A. P. Malozemoff and J. C. Slonczewski, *Magnetic Domain Walls in Bubble Materials*, Applied Solid State Science, Academic Press, 1979.

[21] C. Denis Mee and E. D. Daniel, *Computer Data Storage*, volume 2 of *Magnetic Recording*, McGraw-Hill, 1987, ISBN 0-07-041272-3.

[22] J. Ferré et al., Phys. Rev. B **55**, 15092 (1997).